# DAMAGE MECHANISMS OF ANTICANCER AGENTS: PLATINUM-BASED DRUGS AND COPPER COMPLEXES

A THESIS

SUBMITTED IN PARTIAL FULFILLMENT OF THE REQUIREMENTS

FOR THE DEGREE OF MASTER OF SCIENCE IN

THE GRADUATE SCHOOL OF THE

TEXAS WOMAN'S UNIVERSITY

DEPARTMENT OF CHEMISTRY AND BIOCHEMISTRY

COLLEGE OF ARTS AND SCIENCE

BY

TRANG THI MINH NGUYEN, B.S

DENTON, TEXAS

DECEMBER 2018

## DEDICATION

This thesis is dedicated to my family for supporting me with all affections and love. Thank you dad and mom. You are selfless, work hard, and make scarifies to help my brother, sister, and me accomplish our dreams.

ACKNOWLEDGEMENTS

I would like to acknowledge several people who have helped me in completing this thesis.

First, my honest thanks are to my research advisors, Dr. Nasrin Mirsaleh-Kohan and Dr. Manal Rawashdeh-Omary for teaching and guiding me in research. Also, your recommends are valuable in school and in life. Your encouragement makes my achievement through this process.

Second, I would like to thank my teammate Skylar Wappes for her help. We have had a good time working together in the lab. She is consistently supportive and productive. I would like to recognize Mikaela Wilk, who is a graduate student in Dr. Omary's lab. Although we do not work together in the same lab, Mikaela is willing to help and share experiences.

Third, I would like to thank Dr. Sheardy, who is the Chair of the Department of Chemistry and Biochemistry. He has brought many opportunities for his students to attend conference and present our research posters.

Finally, I would love to thank my "the Nguyen family" and boyfriend for always supporting me spiritually over the years. Your love and jokes are the biggest rewards I could ever have in life. I love you all.

ABSTRACT

TRANG NGUYEN

DAMAGE MECHANISMS OF ANTICANCER AGENTS: PLATINUM-BASED DRUGS AND COPPER COMPLEXES

DECEMBER 2018

Cisplatin and carboplatin, which belong to the platinum based-drugs family, are accustomed to treat various types of cancers. Although they have been used widely in chemotherapy, cisplatin and carboplatin are confronting some issues such as toxicities and drugs resistances. Therefore, designing a new drug without those issues is a challenge. In this study, the technique of Surface-Enhanced Raman Scattering (SERS) is employed in order to research the modification to guanine when cisplatin or carboplatin bound.

The success in clinical use of cisplatin has put metal-based drugs on the first row for cancer treatment. Other than platinum complexes, copper complexes gain major attraction to many scientists. It has been proposed that copper carries less toxic, so copper complexes are potential anticancer agents. Infrared and Raman spectroscopic techniques are engaged to obtain vibrational spectra of copper complexes. Also, SERS technique is utilized to explore the interaction of four new copper complexes with guanine or adenine.

The findings show that when either cisplatin or carboplatin is added to guanine, the guanine spectral changes within the range of 400 and 1800 frequencies. Moreover, new copper complexes also express the guanine or adenine spectral changes in the same range.

TABLE OF CONTENTS

Page

LIST OF TABLES

LIST OF FIGURES

Figure Page

# CHAPTER I

# INTRODUCTION

## INTRODUCTION

Generally, metals are critical for human health. They regulate many biological processes such as activating enzymes, stabilizing protein structures, stimulating hormones, and are involved in redox reaction[1]. The main essential metals found in the human body are Fe, Co, Cu, Zn, Mn, Mo, and Se, which are required for function of enzymes and body growth[1]. A deficiency in any of these metals can lead to disease. For instance, anemia results from either iron deficiency or copper deficiency, selenium deficiency can cause Keshan's disease, and magnesium deficiency is a risk factor for bone and reproductive health[1].

Many metal-based drugs have been utilized to treat diseases or disorders. Vanadium compounds are used to treat diabetes and cancer, lithium compounds are for the treatment of hyperactivity disorder, and gold compounds are known as antiarhtritic agents[2]. Nevertheless, metal-based complexes were of less concern in pharmaceutical application until the discovery of cisplatin, a metal-based drug used in anticancer therapeutic regimens. The successful and extensive practice of using cisplatin has increased the demand of metal-based drugs in cancer research. Scientists have started taking notice of metal-based compounds because they exhibit unique properties such as undergoing redox reactions, alterable DNA binding modes, and reactivity toward the organic substrates of the body[3].

**PLATINUM-BASED DRUGS: CISPLATIN AND CARBOPLATIN**

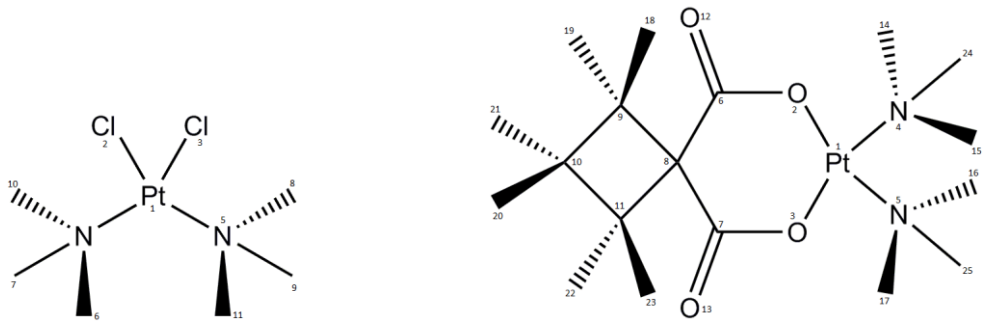


Figure 1. Structure and atom labeling for cisplatin and carboplatin.

*Cis*-diammine-dichloroplatinum(II), or cisplatin (see Figure 1) is introduced as a first generation drug in the platinum-based drug family. It has a noteworthy initiation. In 1844, Michele Peyrone first synthesized cisplatin[4]. In 1893, Alfred Werner proposed the structure of the platinum compound as *trans* and *cis* isomers, and later he won the Nobel Prize for this work[4, 5]. In the 1960s, Barnett Rosenberg, a biophysical professor at Michigan State University, discovered that cisplatin could inhibit cellular division when he was studying the effects of electrical field on *Escherichia coli*. Dr. Rosenberg and colleagues stated that the *cis* geometry was significantly effective in the biological system, while *trans* isomers were ineffective[6,7,8].

The Food and Drug Administration (FDA) approved cisplatin in 1978 for cancer therapy[6]. It has been highly used in treating bladder, cervical, ovarian, lung, esophageal, head, and neck cancers[7]. Although cisplatin is widely used, it induces side effects and drug resistance. When cisplatin is administered into the body intravenously, it affects not only cancer cells, but also most relative normal cell growth and induces toxicities[7]. These toxicities are nephrotoxicity or ototoxicity[6,7]. In addition, information about the drug mechanism is not well understood and scientists face a major challenge to evaluate metal-based drug-DNA interactions.

Since its appearance in clinical use, many anticancer drugs have been developed on the foundation of cisplatin. The goal of a new platinum-based drug is to overcome the disadvantages

of cisplatin. In 1980s, *cis*-diammine(cyclobutane-1,1-dicarboxylato)platinum(II), carboplatin (see Figure 1) was approved by the FDA and presented as second generation in the platinum-based drug family[8]. It was then widely used to fight testicular, ovary, head, neck, and small cell lung cancer[8].

The success of the cisplatin derivative, carboplatin, has mainly been determined by its low toxicity profile[6,7,8,9]. The difference in structure between cisplatin and carboplatin has contributed to different biological performances and relative degrees of toxicity. Cisplatin has two chloride atoms and two amine groups coordinated to the center platinum metal in the *cis* isomer. Chloride atoms are responsible for the biological activity of cisplatin[6,10]. Two chloride atoms are stable because the chloride concentration in blood is high[6,10]. When cisplatin passes through the plasma membrane and enters the cytoplasm, two chloride atoms are lost and replaced by water. Cisplatin then becomes a reactive compound, binds to DNA and form crosslinks[6,10]. This interaction alters the DNA structure[6]. The DNA repair system is incited and recognizes damages. However, if DNA is failed to repair, it triggers cell apoptosis[10].

Carboplatin on the other hand, holds a bidentate dicarboxylate chelate instead of two chlorides leaving ligands. The platinum metal is located inside the ring of carboplatin[18]. Despite bidentate dicarboxylate ligands being displaced before binding to DNA in carboplatin as same as cisplatin, carboplatin has a slower hydrolysis reaction rate which is equivalent to about two orders of magnitude than cisplatin[12].

Although carboplatin is recognized to be less toxic than cisplatin, the binding of either cisplatin or carboplatin can produce lesions to DNA. The interstrand crosslink contributes 5-10% of the DNA-drug binding, but it has the most cytotoxic effect[11].

## COPPER COMPLEXES

Copper is a bio-essential transitional metal element. Its distribution is mostly found in the liver, heart, spleen, kidneys, brain, and blood concentrated in the pigmented parts of the eyes[13,14]. A healthy human adult of 70 kg can contain a total of 80-120 mg of copper[13,14]. Copper has two oxidation states, Cu (I) and Cu (II). Cu (I) tends to be colorless, and its complexes are either a linear or tetrahedral coordination. Cu (II) tends to be green or blue color, and its complexes are square planar, distorted octahedral, and distorted tetrahedral[13]. Biological roles of copper involve redox reactions, oxygenations, and $O_2$-carrying proteins[13,14,15]. Some studies have shown that copper can execute its role as an antioxidant and a pro-oxidant[14,15]. Also, various enzymes require copper to maintain activity and build molecular structures such as tyrosinase, amine oxidases, ascorbate oxidase, and superoxide dismutase[13,15]. As stated above, copper deficiency leads to blood effects[1].

Copper complexes have shown potential in medical treatment. Copper complexes possess anti-inflammatory activity depending on dose and route of administration[16]. Markedly, the mechanisms of anti-inflammatory activity of copper complexes have been reported as inducing lysyl oxidase activity, modulating prostaglandin synthesis, inducing or mimicking superoxide dismutase activity, decreasing the permeability of human synovial lysosomes, and modulating the physiological effects of histamine [17]. Moreover, copper complexes possess other potential use such as antimicrobial, antiviral, anticancer, enzyme inhibitors, or chemical nuclease[18]. For example, the copper (II) complex of 3,5-diisopropylsalicylate has attracted a great interest among pharmacology research[19].

Many new copper complexes have shown their prospective antitumor properties. Among the metal complexes, copper complexes that are believed to be less toxic than cisplatin have a different mechanism of action, and a broader spectrum of antitumor activity[14]. However, there is

limited information about these circumstances. Ligands and donor atoms determine DNA binding affinity of copper compounds[14]. Likewise, the geometry of copper-coordinated compounds allows them to easily interact with DNA helix compare to other metals[20]. Since the discovery of Sigman in 1979, copper-1,10-phemanthroline complexes have become an extensive attraction for many researchers because of its chemical nuclease activity to DNA[21].

**DRUG-DNA INTERACTION**

DNA is the major target of anticancer drugs. DNA binding modes of drugs are sorted into intercalating, grove-binding, covalent bonding, and strand breaking[22].

Intercalation is the well-known mode of DNA-drugs interaction. It is identified by the insertion of drugs between the stacked base pairs of the DNA double helix[22,23]. The intercalating agents contain a polycyclic aromatic ring[22]. This interaction is held by van der Waals force between the π-electron system and nucleobases[22]. When the intercalation process happens on either the minor or major groove, two base pairs are separated largely and the DNA helix becomes prolonged and distorted by the unwinding of the duplex[23]. Platinum based-drugs demonstrate multiple binding sites to form either intrastrand or interstrand[6,11]. The difference of binding site will result in the difference in cytotoxicity and biological activity among the drugs[22].

Two DNA backbones run in opposite directions. When the angle between two backbones is large, the major groove occurs. When the angle between two backbones is small, the minor groove occurs. Yet, minor groove binding is the main focus in the research of anticancer drugs[24].

Most anticancer drugs covalently bind to DNA bases[22]. Cisplatin and other platinum derivatives exhibit covalent binding to DNA. Alkylating agents attach to the base of DNA and form adducts at the N7 position of the purine ring[6,10,23]. The adducts formed by platinum-based drugs and DNA are 1,2-d(GpG intrastrand crosslinks, 1,2-d(ApG) intrastrand crosslink, 1,3-intrastrand crosslink, interstrand crosslink, and monofunctional adduct[6,11]. The dominant adduct is

the 1,2-intrastrand crosslink, but only the interstrand crosslink retains anticancer purpose[11]. The significant prevalence of cisplatin binds to guanine over adenine has been proved[25]. This is due to the missing of hydrogen bonding between the $NH_3$ on cisplatin complex and O6 position in adenine[23].

Cleavage of DNA can be distinguished to oxidative pathway or hydrolysis of phosphoester linkages[26]. DNA cleavage property is seen among copper complexes, especially copper-1,10-phenanthroline has been informed[20,26,27,28]. The *bis*(phen)copper(I) complex cleaves DNA in the presence of $H_2O_2$ and a thiol[26,27,28].

**OBJECTIVES**

This research aims to address three objectives. First, the influence of pH on guanine will be studied by Surface-Enhanced Raman Scattering (SERS) techniques. The SERS spectra of guanine at physiological and alkaline pH will be observed and compared. Second, the interaction of cisplatin and carboplatin on guanine will be investigated by SERS techniques. The examination will give a better understanding of both drugs binding actions. Accordingly, promised platinum-based drugs that are less toxic and more efficient can be designed. Third, four new copper complexes were synthesized in Dr. Omary's lab by a graduate student. Their properties will be characterized by various spectroscopic techniques, namely, Raman spectroscopy, UV-visible absorption, and infrared (IR) spectroscopy. The binding behaviors of the copper complexes will be evaluated through the interaction with guanine and adenine. The success of this study will put copper complexes as potential anticancer agents because they are inexpensive and have less toxicity compared to cisplatin. SERS will be employed in the study of the interaction of copper complexes and DNA bases. SERS is a powerful technique in the analytical research because it enhances signals more than normal Raman. It is a non-destructive technique for delivering structural and binding information of an analyte at low concentration.

# CHAPTER II

# SPECTROSCOPIC PRINCIPLES

## RAMAN VS. IR SPECTROSCOPY

Raman spectroscopy is an analytical technique in the field of vibrational spectroscopy. An Indian scientist, named C.V. Raman, invented Raman spectroscopy[29]. In Raman spectroscopy, the vibrational transitions occur due to the scattering of light by molecules. Two types of light scattering can arise in a molecule, Rayleigh scattering and Raman scattering. Figure 2 illustrates the differences of Rayleigh scattering and Raman scattering. Rayleigh scattering is elastic scattering. It results in the collision between a photon and a molecule with no change in energy or frequency of light. Contrarily, Raman scattering is inelastic scattering. It has either greater or less energy than the incident light. The most common scattering that occurs in nature is Rayleigh scattering (>>99%), while Raman scattering is less predominant (<<1%). When the light is scattered and most of the photons are shifted to a longer wavelength (lower energy), it is called Stokes shift. Some photons are shifted to a shorter wavelength (higher energy), this is called anti-Stokes shift. Both of the shifts can be mathematically expressed as:

$$E = h\nu \pm \Delta E$$

E is energy, h is plankton's constant, $\nu$ is wavenumber; $\Delta E$ is the change in energy from vibrational state to ground state[29].

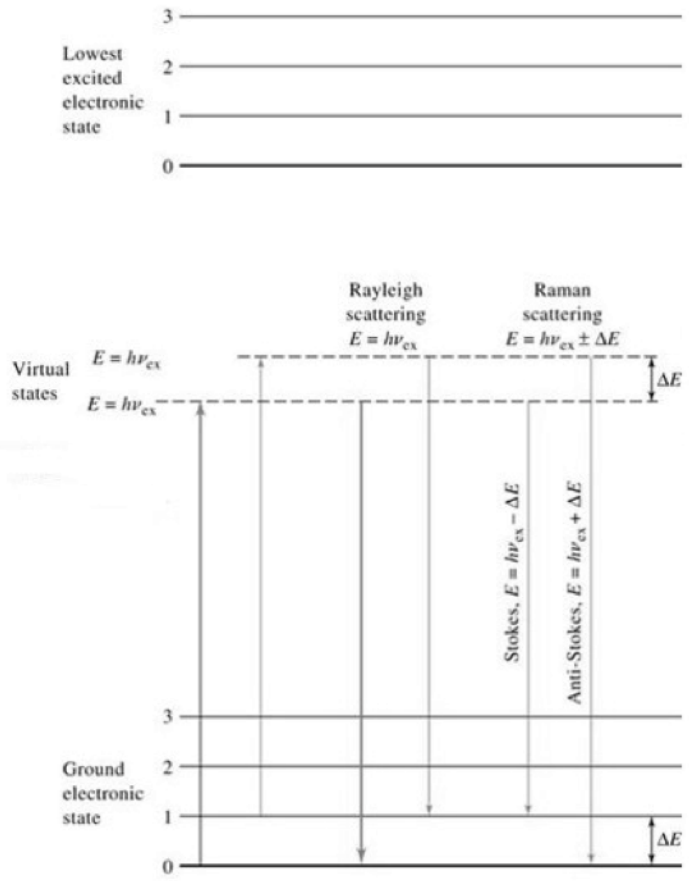


Figure 2. Schematic representation of the Raleigh and Raman scattering[29].

IR spectroscopy is another type of vibrational spectroscopy. In IR spectroscopy, the vibrational transitions occur due to the absorption of light in the infrared region by molecules. Raman spectroscopy is complimentary to IR absorption spectroscopy. However, there are some differences between these because of the different selection rules. Raman spectroscopy shows the change in polarizability of a molecule, whereas IR spectroscopy shows the change in dipole moment. Therefore, if a vibrational mode is IR active, it is Raman inactive and vice versa[29]. The sample experienced in Raman spectroscopy can be in liquid or solid form, but water causes interference in IR spectroscopy. Raman spectroscopy provides information on crystal structure, while IR spectroscopy provides information on functional groups and bonds in the molecule[29].

## SURFACE-ENHANCED RAMAN SPECTROSCOPY

Raman scattering usually shows a weak intensity, so a sensitive and selective spectroscopic technique, Surface-Enhanced Raman Scattering (SERS) is employed to improve the shortcoming. SERS is achieved when an analyte is absorbed onto a metal surface. Consequently, when the light radiation interacts to metal, the surface electrons are excited and produce plasmon resonance. The Raman signals are enhanced by a factor of $10^{6}$[30]. SERS substrate is the major point to deliver the largest enhancement. It can reach to the factor of $10^{10}$ – $10^{11}$[30,31]. Silver and gold metals, especially nanostructures with dimensions less than 100 nm are considered as a good rough surface for SERS experiments[30]. Comparing to Raman spectra, SERS spectra show more resolved peaks at higher intensity. The sample of SERS can be attained at a low concentration[30].

The SERS enhancement factors are contributed to the electromagnetic enhancement factor and chemical enhancement factor[30,31]. The electromagnetic mechanism regards to the increasing of electric field on a metal surface caused by localized surface plasmon. The chemical mechanism regards to the increased of molecular polarizability caused by charge-transfer complex between a metal surface and an analyte. The enhancement factor of SERS is described in the below equation:

$$\mu = \alpha E$$

$\alpha$ is chemical enhancement. E is electromagnetic enhancement[30,31].

## UV-VIS SPECTROSCOPY

When the ultraviolet and visible radiations interact with matter, electronic transitions occur in the outer electrons of molecules[29]. These electrons are $\pi$ electrons, which are associated with double bonds[29]. UV-Vis spectroscopy is identified as a simple and common technique for study the DNA concentration and DNA-drugs interaction. This technique gives out the

information about the absorption properties of the DNA molecules or drug complexes in the UV region ($\pi \rightarrow \pi^*$ intra-ligand transitions or ligand-to-metal charge transfer) or visible region ($d \rightarrow d$ transitions)[29]. Figure 3 shows the energy levels of electronic transitions. Typically, the absorption peak of free metal complexes is compared to the absorption peak of metal complexes bound DNA. Any shifting between those two peaks shows an interaction. The UV-Vis spectroscopic study requires the presence of water. Normally, the absorption spectrum of DNA has a broad range of 200-350 nm, where the maximum absorption is at 260 nm[32]. The nitrogenous bases of DNA are easily protonated; the peak can be changed in the function of pH[32]. The concentration of DNA can be calculated following Beer's Law:

$$A = \varepsilon lc$$

A is absorption, ε is molar extinction coefficient, l is path length of sample cell, c is molar concentration[29].

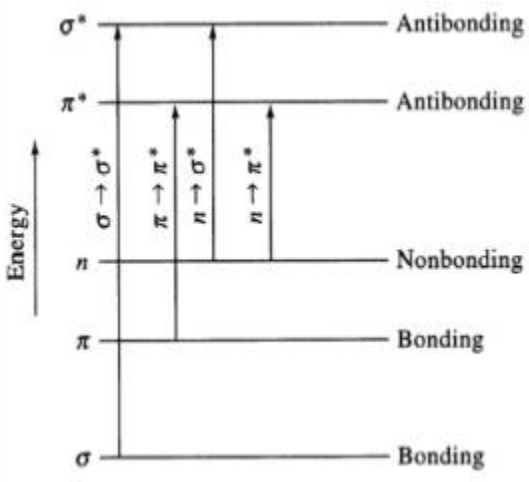

Figure 3. Schematic representation of the electronic transitions[29].

# CHAPTER III

# METHODOLOGY

## PREPARATION OF SILVER NANOPARTICLES

The enhanced signal of SERS depends on the optical behaviors of nanoparticles. These properties include scattering and absorption. Although nanoparticles can be synthesized in a wide range of shapes and sizes, the aggregated nanoparticles in the sample is crucial in order to measure good enhancement. In this research, silver nanoparticles were used as a metal surface and synthesized basing on the protocol of Lee and Meisel[33].

The procedure of making silver nanoparticles involves two parts. First part is glassware cleaning. The flask is used to synthesize and brown bottle is used to store the silver nanoparticles. Aqua regia is prepared to remove all residual. 300 mL of hydrochloric acid HCl (Fisher Scientific Lot # 126384) and 100 mL of nitric acid $HNO_3$ (Fisher Scientific Lot # 126384) are combined in a 500 mL flask along with a stir-bar. The flask is left under the fume hood and soaked for three hours. After three hours, aqua regia is poured slowly into a brown bottle. Aqua regia must be diluted and then emptied down to the sink that has been covered with baking soda $NaHCO_3$. The flask, brown bottle, and stir-bar should be rinsed with ultra-pure water for four times. Second part is nanoparticle production. 200 mL of ultra-pure water is added into clean 500 mL flask and heated up. 45 mg of silver nitrate $AgNO_3$ (Fisher Scientific Lot # 110502) is added to the flask. The water does not have to be boiling when silver nitrate was being added. Once the water is boiling, 50 mg of sodium citrate $Na_3C_6H_5O_7$ (Spectrum Chemical Lot # TV1335) is added. The mixture is continuing to boil for 45 minutes until the color of solution is changing from clear to milky-gray. The solution should be cooled before transferring to brown bottle. The final volume of nanoparticle solution in brown bottle is brought to 400 mL by filling up with ultra-pure water.

The final product could be stored for two months and was approximately 35 nm in diameter. The nanoparticle solution does not produce a symmetric vibration in Raman spectroscopy.

**PREPARATION OF AGGREGATION AGENT**

SERS enhancement factor highly depends on an aggregation agent. It is experimentally observed from the aggregation of colloids. Magnesium sulfate $MgSO_4$ was chosen for this SERS study. The salt does not have the Raman spectrum in the DNA region 400 – 1800 $cm^{-1}$. The salt solution was prepared by dissolving powder of magnesium sulfate to ultra-pure water to get the final concentration 0.2 M.

**PREPARATION OF SERS SAMPLES**

**Part A Materials.** Cisplatin was purchased from Acros (Lot # A0344932) with 99.99% purity, while carboplatin were purchased from Tokyo Chemical Industry Co., Ltd (TCI) in America (Lot # Q5WLJ-LG) with > 98.0% purity. Guanine was purchased from Acros (Lot # A0328346) with 99+%.

**Part B Materials**. Four new copper complexes were synthesized from Tetrakis(acetonitrile)copper(I) tetrafluoroborate and 1,10-phenanthroline in acetonitrile in Dr. Omary's lab. Guanine was purchased from Acros (Lot # A0328346) with 99+% purity. Adenine was purchased from Acros with 99% purity (Lot # A0333101).

**Methods.** SERS samples were prepared in the borosilicate glass (maximum capacity of 1.5 mL and thickness of 1mm). The analyte were prepared all in liquid form. The powders of drugs or DNA bases were dissolved in ultra-pure water at certain concentration. The protocol will be described in detail in each chapter. The solution was then vortexed to completely dissolve to make the stock solution. An aggregating agent as $MgSO_4$ was used to promote cluster formation. The order of materials matters in order to obtain an effective SERS sample. Figure 4 illustrates the process of making SERS samples. SERS sample of drugs or DNA bases by itself did not

involve incubating process, but SERS sample of drugs and DNA bases together must be incubated at 37°C for 24-48 hours before adding nanoparticles and salt.

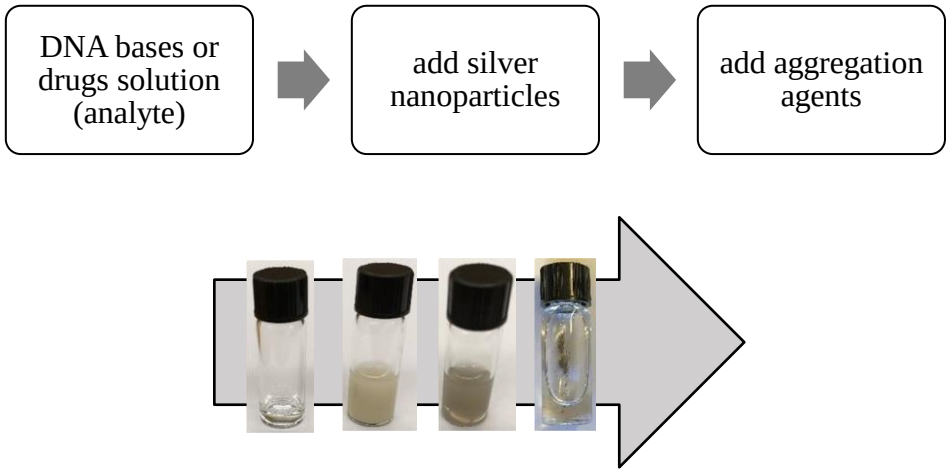


Figure 4. Schematic diagram for the preparation of SERS samples.

CHAPTER IV

# SURFACE-ENHANCED RAMAN SPECTROSCOPIC STUDIES OF GUANINE IN VARIOUS PH CONDITIONS

## OVERVIEW

Guanine (Molecular formula: $C_5H_5N_5O$) is a base found in nucleic acids. It is composed of a six-carbon pyrimidine ring fused with a five-carbon imidazole ring and a conjugated double bond (see Figure 5). Guanine is structured into a square-planar configuration.

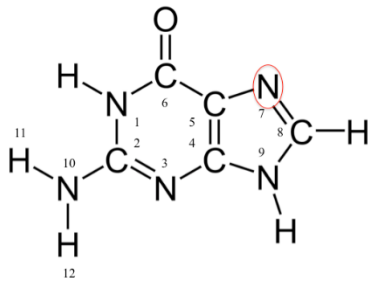

Figure 5. Structure and atom labeling for guanine.

SERS spectra of guanine absorbed to colloidal silver particles have been published previously[34, 35]. Guanine was chosen for the experiment because it is highly preferred by cisplatin. Specifically, the N7 position on guanine is the primary binding target of cisplatin[6,10,23,34,35] and plays a critical role for the antitumor property of cisplatin. At this location, cisplatin attacks the DNA strand and makes crosslinks to an adjacent purine. Such crosslinks, interstrand crosslinks in particular, distorts DNA [6,10,11]. This leads to stopping DNA replication and ultimately kills the cells.

The SERS guanine was examined first in this study that preceded the SERS investigation of guanine in the presence of drugs. The purpose of this study is to interpret the conformational changes of DNA bases as a function of pH. Guanine exists in two tautomeric forms, keto and

enol. It turns to keto form under physiological pH[36]. However, when guanine interacts to silver colloids, the pKa of guanine reduces to 0.5[34]. SERS spectra of guanine at various pH conditions are reported in this work to give full understanding about the interaction of guanine with surface substrates.

## EXPERIMENTAL

Guanine solution was prepared by dissolving guanine powder with ultra-pure water. The stock solution was at pH 8 and $10^{-4}$ M. In order to obtain a guanine solution at biological pH, HCl was added to the stock solution to adjust to pH 7. The SERS samples of guanine were made by combining guanine solution, silver nanoparticles, and 0.2 M $MgSO_4$. The SERS of guanine could not be successful without the addition of an aggregation agent. The final volume in each vial was 1000 μL. The sample vials were set aside for 1-2 hours before the scans were collected to ensure proper aggregation occurred. In order to obtain the guanine samples at alkaline pH, a solution of sodium hydroxide was added to adjust the pH. The concentration of guanine samples was also kept at $10^{-4}$ M and 0.2 M of $MgSO_4$ was still used to help aggregation.

## SERS OF GUANINE AT PH 7 VS. PH 8

This first project began with examining the influence of biological pH to guanine. Although there are some publications, this work was important as a basis for the study of drug-DNA interaction[34,35]. The results of guanine at biological pH are illustrated in Figure 6 and Table 1. Basing on the SERS scans, we only obtain the position of the peaks and its existence, not the intensity.

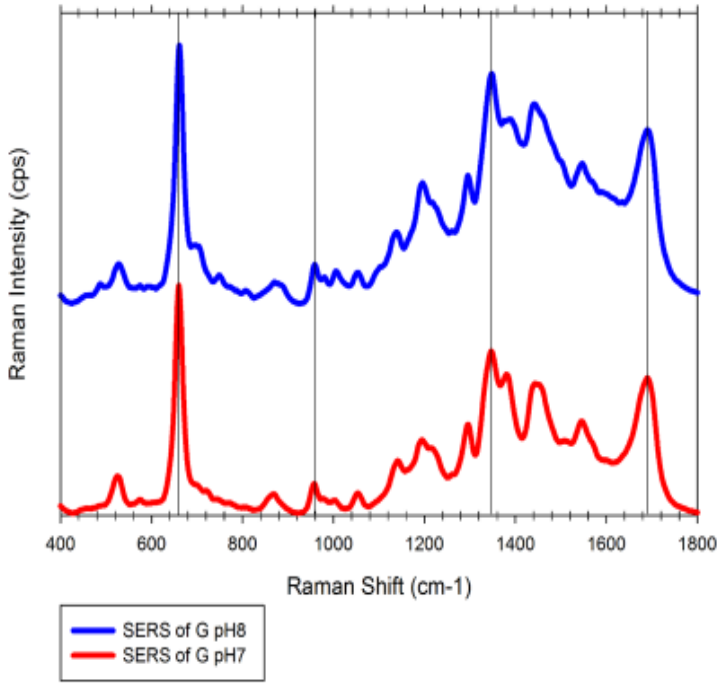


Figure 6. Surface-enhanced Raman spectrum of guanine was obtained at pH 8 (blue) and pH 7 (red); excitation laser, 780 nm; exposure time, 3 s; guanine concentration, $10^{-4}$ M.

**Table 1. Raman Shift Values from SERS Spectra of Guanine at pH 8 and pH 7 within 5 $cm^{-1}$ resolutions.**

| **Raman shift ($cm^{-1}$)** | | |
|---|---|---|
| **Guanine pH 8** | **Guanine pH 7** | **Δ shift** |
| 527.91 | 524.30 | 3.61 |
| 660.97 | 660.25 | 0.72 |
| 870.21 | 868.53 | 1.68 |
| 958.92 | 957.24 | 1.68 |
| 1053.42 | 1053.66 | -0.24 |
| 1138.27 | 1141.41 | -3.14 |
| 1196.12 | 1194.44 | 1.69 |
| 1295.44 | 1295.68 | -0.24 |
| 1348.47 | 1346.79 | 1.69 |
| 1388.01 | 1380.54 | 7.47 |
| 1440.07 | 1443.21 | -3.14 |
| 1547.10 | 1545.42 | 1.69 |
| 1689.81 | 1690.05 | -0.24 |

In Figure 6, SERS of guanine at pH 7 and pH 8 are compared graphically. Table 1 shows the Raman shifts for guanine at these pH levels. The blue spectrum represents SERS of guanine at pH 8 and the red spectrum represents SERS of guanine at pH 7. Approximately 12 well-defined peaks occur in the region 400 – 1800 $cm^{-1}$. There are similarities and slight differences between pH 7 and pH 8. Slight shifts are observed. Most of which are less than 4 $cm^{-1}$. The carbonyl stretching band is suggested to happen in the region 1500 – 1900 $cm^{-1}$. Actually, the guanine carbonyl stretching bands are observed at 1690 $cm^{-1}$ in both pH solutions. It shows a strong enhancement signal but no respective shift. The signal of symmetric ring breathing mode at 660 $cm^{-1}$ is very strong. The ring deforming modes at 525 $cm^{-1}$ and 870 – 960 $cm^{-1}$ are different. After adjusting the pH, these deforming modes are noticeably blue shifts. There is a small "hump" developing in pH 8, but it does not show up in pH 7. Unlike the SERS spectrum of guanine at pH 8, SERS spectrum of guanine at pH 7 does not show comparable signals at 700 – 750 $cm^{-1}$. The SERS signal of guanine at pH 8 and pH 7 at 1380 $cm^{-1}$ has visible differences. At pH 8, the peak shows at 1388 $cm^{-1}$, while the peak is a blue shift to 1380 $cm^{-1}$ at pH 7. The $\Delta$ shift is around 7.5 $cm^{-1}$. This is the only shift that is greater than the resolution.

**SERS OF GUANINE AT BIOLOGICAL PH VS. ALKALINE PH**

In the second part of guanine studies, the effect of alkaline pH such as pH 9 and pH 11 on guanine were taken. The N1 and N9 positions of guanine have pKa around 9.65 and 10.03, respectively[36]. When the pH is higher than pKa, the base will be deprotonated and its charge will be negative. The deprotonation can takes place at the N1and N9 position at pH 11[35].

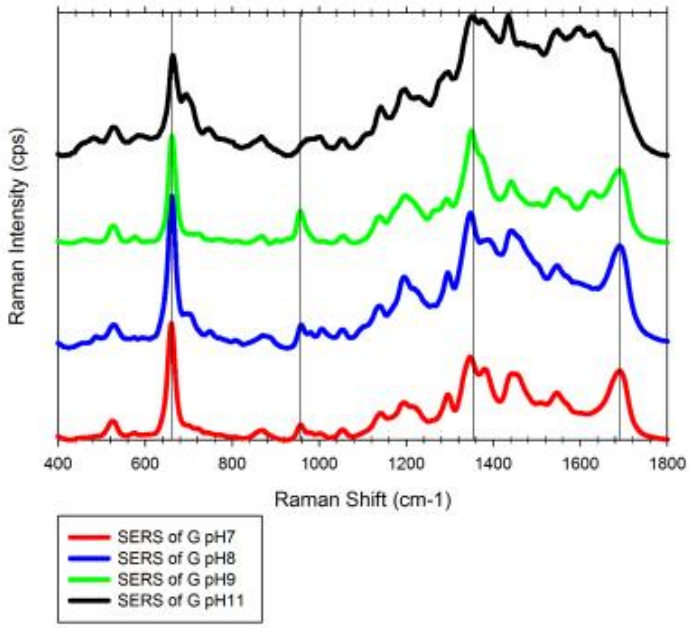


Figure 7. Surface-enhanced Raman spectrum of guanine were obtained at pH 7 (red), pH 8 (blue), pH 9 (green), pH 11 (black); excitation laser, 780 nm; exposure time, 30 s; guanine concentration, $10^{-4}$ M.

**Table 2. Raman Shift Values from SERS Spectra of Guanine at pH 7, pH 8, pH 9, and pH 11 within 5 $cm^{-1}$ resolutions and Assignment to Vibrations of the Guanine Molecule (Based on Reference 35).**

| Raman shift ($cm^{-1}$) | | | | | Assignments [35] |
|---|---|---|---|---|---|
| **Guanine pH 7** | **Guanine pH 8** | **Guanine pH 9** | **Guanine pH 11** | **Δ shift (pH 7 vs. pH 11)** | |
| 524.30 | 527.91 | 525.85 | 529.10 | 4.80 | Deforming R6 (squeezing C6N1C2, N3C4C5) |
| 660.25 | 660.97 | 661.14 | 663.40 | 3.15 | Breathing R6 |
| 868.53 | 870.21 | 867.91 | 867.53 | -1.00 | Wagging $NH_2$, Deforming R6 (squeezing N1C2N3), R5 (squeezing C8N9C4) |
| 957.24 | 958.92 | 956.18 | N/A | N/A | Deforming R5 (squeezing group N7C8N9) |
| 1053.66 | 1053.42 | 1054.70 | 1050.43 | -3.23 | Stretching N1C2+C2N10 |
| 1141.41 | 1138.27 | 1138.27 | 1141.84 | 0.43 | Rocking $NH_2$, stretching C6N1 |
| 1194.44 | 1196.12 | 1197.64 | 1197.52 | 3.08 | Rocking $NH_2$, bending N1H, C8H |
| 1295.68 | 1295.44 | 1293.58 | 1296.77 | 1.09 | Bending C8H, N1H, stretching N7C8, rocking $NH_2$, N10H12 |
| 1346.79 | 1348.47 | 1349.90 | 1349.97 | 3.18 | Bending C8H, stretching C4N9+C5C6+N7C8 |
| 1380.54 | 1388.01 | N/A | N/A | N/A | Bending N1H, C8H, stretching N3C4-C4C5+N1C2-N7C8 |
| 1443.21 | 1440.07 | 1441.14 | 1434.35 | -8.86 | Stretching N1C2-N3C4+C4C5-C6O, bending N1H |
| 1545.42 | 1547.10 | 1544.19 | 1547.32 | 1.90 | Scissoring $NH_2$, stretching C2N3-C2N10, bending N1H |
| 1690.05 | 1689.81 | 1688.41 | N/A | N/A | Stretching C60-C5C6-C2N3, bending N1H |

The SERS spectra of guanine at neutral pH and alkaline pH are compared and graphed in Figure 7. The assignments of vibration bands of N1-deprotonated and N9-deprotonated are summarized in Table 2. The frequencies of SERS along with the assignments are based on the published Density Functional Theory (DFT) report[35]. The Δ shift was calculated by two extreme pH differences. The region at 525 $cm^{-1}$, 660 $cm^{-1}$, and 870 $cm^{-1}$ do not display particular shifts. It is important to realize that a hump at 700 $cm^{-1}$ is seen at pH 8 and 11. Around 957 $cm^{-1}$ regions do not express a defined peak. It is noticed that the clusters from 1380 $cm^{-1}$ to 1800 $cm^{-1}$ show the differences when adjusting the pH. The peak at 1380 $cm^{-1}$ shows up in both pH 7 and pH 8, but it disappears at pH 9 and pH 10. Only pH 11 shows the most shifts at 1440 $cm^{-1}$. A defined peak at 1690 $cm^{-1}$ does not exist or shifts to the left. Also, there is a slight shift of guanine at pH 9 and a large shift at pH 11 compared to guanine at neutral pH. The blue shifts are seen between the spectra as pH increases. These shifts are the carbonyl-stretching band, which are above 1690 $cm^{-1}$ of guanine spectrum at alkaline pH. When pH 7 and pH 11 are compared, only the shift at 1440 $cm^{-1}$ is found to consider for stretching and bending at the N1 position.

**CONCLUSION**

This study has shown that use of a SERS technique is adequate for getting quality SERS spectrum of guanine since the molecules are absorbed directly on the metal surface. The method allows the Raman scattering to be enhanced, while the concentration of the solution is low. The scattered radiations are improved to such a large enhancement factor because of the high electromagnetic field. All the experiments were assimilated at a wavelength of 780 nm.

In summary, the SERS spectra of guanine at different pH are compared and reported. New peaks and shifts are noticeable. It is concluded that the SERS spectrum of guanine at pH 8 shows the most resolved and distinct peaks comparing to the other pH. At biological pH, the six-carbon ring breathing, bending at the C8 position, and stretching at the C6 position are strong

modes. At alkaline pH, some peaks at 960 $cm^{-1}$, 1380 $cm^{-1}$, and 1690 $cm^{-1}$ are not visible. The five-carbon ring deformation and bending at the N1 position could occur in a function of pH.

# CHAPTER V

# SURFACE-ENHANCED RAMAN SPECTROSCOPIC STUDIES OF PLATINUM DRUGS MODIFICATION TO GUANINE

## OVERVIEW

As stated above, the N7 position on guanine is significant for the binding of platinum drugs[6,10,23,34,35]. The platinum drugs are required to be aqua species before they can make any attachment to DNA. The DNA adducts are formed between purine residues in the same or opposite strand[6,37]. Although interstrand crosslinking is a minor adduct, it holds the anticancer property. A previous Raman spectroscopic study indicated that carboplatin DNA cross-link adducts are similar to cisplatin adducts[38]. The most effective adduct is known as the interstrand crosslinks[11]. The structural differences between cisplatin and carboplatin lead to the reaction rate differences[12]. Therefore, it results in the substantial differences in toxicity and efficacy of each drug in cancer remedy. Carboplatin is reported as less likely to produce toxicity when it is carried out at high dose chemotherapy than cisplatin[9]. Both cisplatin and carboplatin possess a broad spectrum in clinical interest, but carboplatin can substitute cisplatin in some type of tumors such as ovarian cancer cells[9]. The mechanistic study of the interaction of platinum drugs and DNA bases is very critical for better understanding their binding behavior and improving the side effects. For that reason, the experiments are focused on examining the binding of guanine to cisplatin and carboplatin.

## EXPERIMENTAL

The studies of platinum-guanine complexes were conducted by SERS near physiological pH. To prepare the SERS samples, the stock solution of cisplatin or carboplatin and guanine were prepared with concentration of $10^{-4}$ M and pH was adjusted around 7-8, basing on the biological

system. The 1:1 and 5:1 DNA bases to drugs molar ratio and 24 hours and 48 hours incubation periods were attempted in this research. 500 µL of silver nanoparticles and 200 µL of 0.2 M of $MgSO_4$ were then added to each vial after incubation period. The scans for all samples were collected within 2 hours.

**SERS OF CISPLATIN MODIFICATION TO GUANINE**

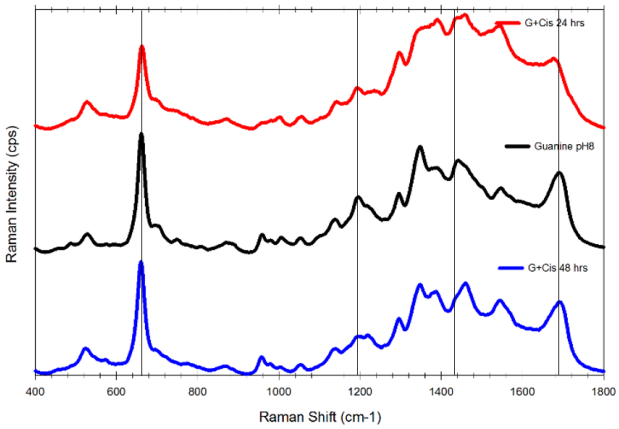


Figure 8. Surface-enhanced Raman spectrum of guanine was obtained at pH 8 (black), after incubation with cisplatin (5:1 ratio) for 24 hours (red) and 48 hours (blue); excitation laser, 780 nm; exposure time, 3 s; guanine concentration, $10^{-4}$ M; cisplatin concentration $10^{-4}$ M.

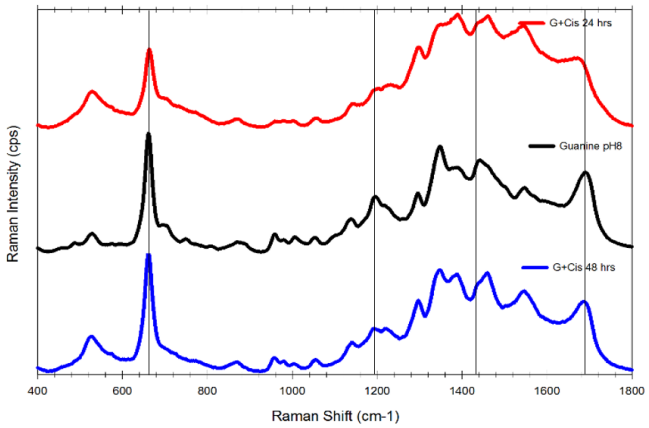


Figure 9. Surface-enhanced Raman spectrum of guanine was obtained at pH 8 (black), after incubation with cisplatin (1:1 ratio) for 24 hours (red) and 48 hours (blue); excitation laser, 780 nm; exposure time, 3 s; guanine concentration, $10^{-4}$ M; cisplatin concentration $10^{-4}$ M.

**Table 3. Raman Shift Values from SERS Spectra of Guanine at pH 8 and after incubation with cisplatin (5:1 ratio) within 5 $cm^{-1}$ resolutions and Assignment to Vibrations of the Guanine Molecule (Based on Reference 39).**

| Raman shift ($cm^{-1}$) | | | | | Assignments [39] |
|---|---|---|---|---|---|
| **Guanine** | **G+Cis 5:1 24hrs** | **Δ shift** | **G+Cis 5:1 48hrs** | **Δ shift** | |
| 527.91 | 526.94 | -0.96 | 524.05 | -3.86 | Deforming R6 (squeezing C6N1C2, N3C4C5), deforming R6 (squeezing C5C6N1, C2N3C4) |
| 660.97 | 661.94 | 0.96 | 660.01 | -0.96 | Breathing R6, wagging N1H |
| 870.21 | 871.18 | 0.96 | 869.25 | -0.96 | Def R5 (squeezing C4N9C8, stretching C5N7), R6 (squeezing N1C2N3) |
| 958.92 | N/A | N/A | 956.99 | -1.93 | Deforming R5 (squeezing N7C8N9), stretching PtN7 |
| 1053.42 | 1056.31 | 2.89 | 1052.45 | -0.96 | Rocking $NH_2$, C2N3-C6N1, bending N9H, C8H, stretching C8N9, stretching N1C2 |
| 1138.27 | 1143.09 | 4.82 | 1139.23 | 0.96 | Stretching C6N1-C4N9, rocking $NH_2$ |
| 1196.12 | 1191.30 | -4.82 | 1196.12 | 0.00 | Stretching PtN7 + C6N1 + C4N9, bending C8H, N9H, stretching C5N7, deforming R6 (squeezing N3C4C5) |
| 1295.44 | 1296.40 | 0.96 | 1295.44 | 0.00 | Bending N1H, stretching C5N7-C5C6-C2N10-N3C4, deforming $NH_3$ |
| 1348.47 | 1350.40 | 1.93 | 1348.47 | 0.00 | Stretching C5N7-C5C6 + C4N9 + C2N10(-N3C4), bending N1H, deforming $NH_3$ |
| 1388.01 | 1390.90 | 2.89 | 1386.08 | -1.93 | Stretching N1C2 + C4N9-C4C5(+N7C8), bending N1H, bending N9H, stretching C8N9-C5N7 |
| 1440.07 | 1458.39 | 18.32 | 1460.32 | 20.25 | Stretching N7C8 + N1C2-C4N9-C6O-C5C6, scissoring $NH_2$, bending C8H, N1H, stretching N7C8-N1C2 + C6O |
| 1547.10 | 1546.14 | -0.96 | 1545.18 | -1.93 | Scissoring $NH_2$, stretching C2N10-C2N3 |
| 1689.81 | 1676.31 | -13.50 | 1690.78 | 0.97 | Stretching C6O-C5C6, bending N1H, deforming $NH_3$ |

**Table 4. Raman Shift Values from SERS Spectra of Guanine at pH 8 and after incubation with cisplatin (1:1 ratio) within 5 $cm^{-1}$ resolutions and Assignment to Vibrations of the Guanine Molecule (Based on Reference 39).**

| Raman shift ($cm^{-1}$) | | | | | Assignments [39] |
|---|---|---|---|---|---|
| **Guanine** | **G+Cis 1:1 24hrs** | **Δ shift** | **G+Cis 1:1 48hrs** | **Δ shift** | |
| 527.91 | 527.91 | 0.00 | 526.94 | -0.96 | Deforming R6 (squeezing C6N1C2, N3C4C5), deforming R6 (squeezing C5C6N1, C2N3C4) |
| 660.97 | 662.90 | 1.93 | 660.97 | 0.00 | Breathing R6, wagging N1H |
| 870.21 | 864.43 | -5.79 | 870.21 | 0.00 | Def R5 (squeezing C4N9C8, stretching C5N7), R6 (squeezing N1C2N3) |
| 958.92 | 958.92 | 0.00 | 956.99 | -1.93 | Deforming R5 (squeezing N7C8N9), stretching PtN7 |
| 1053.42 | 1057.27 | 3.86 | 1053.42 | 0.00 | Rocking $NH_2$, C2N3-C6N1, bending N9H, C8H, stretching C8N9, stretching N1C2 |
| 1138.27 | 1140.20 | 1.93 | 1141.16 | 2.89 | Stretching C6N1-C4N9, rocking $NH_2$ |
| 1196.12 | 1204.80 | 8.68 | 1193.23 | -2.89 | Stretching PtN7 + C6N1 + C4N9, bending C8H, N9H, stretching C5N7, deforming R6 (squeezing N3C4C5) |
| 1295.44 | 1296.40 | 0.96 | 1296.40 | 0.96 | Bending N1H, stretching C5N7-C5C6-C2N10-N3C4, deforming $NH_3$ |
| 1348.47 | 1350.40 | 1.93 | 1348.47 | 0 | Stretching C5N7-C5C6 + C4N9 + C2N10(-N3C4), bending N1H, deforming $NH_3$ |
| 1388.01 | 1389.93 | 1.93 | 1387.04 | -0.96 | Stretching N1C2 + C4N9-C4C5(+N7C8), bending N1H, bending N9H, stretching C8N9-C5N7 |
| 1440.07 | 1460.32 | 20.25 | 1459.36 | 19.29 | Stretching N7C8 + N1C2-C4N9-C6O-C5C6, scissoring $NH_2$, bending C8H, N1H, stretching N7C8-N1C2 + C6O |
| 1547.10 | 1544.21 | -2.89 | 1546.14 | -0.96 | Scissoring $NH_2$, stretching C2N10-C2N3 |
| 1689.81 | 1663.78 | -26.03 | 1685.95 | -3.86 | Stretching C6O-C5C6, bending N1H, deforming $NH_3$ |

The SERS spectra of cisplatin and guanine complexes with different conditions such as ratio and incubation times were collected. Figure 8 shows the comparison between the SERS spectrum of guanine and the SERS spectrum of guanine upon adding cisplatin (5:1 ratio) after 24 hours and 48 hours incubation time. Table 3 gives the Raman shift and peak assignments of Figure 8. Figure 9 shows the comparison between the SERS spectrum of guanine and the SERS spectrum of guanine upon adding cisplatin (1:1 ratio) after 24 hours and 48 hours incubation time. Table 4 gives the Raman shift and peak assignments of Figure 9.

As seen in Figures 8 and 9, the SERS spectra of cisplatin and guanine complexes show relative spectral changes particularly in the region 400 – 1800 $cm^{-1}$. The distinct peak at 660 $cm^{-1}$, 958 $cm^{-1}$, and 1350 $cm^{-1}$ of red line seems to have fewer enhancements and is likely to disappear. A cluster that is from 960 $cm^{-1}$ to 1700 $cm^{-1}$ shows noticeable differences. In this experiment, intensity is not involved in the analysis because it is contingent on the focus of laser and the amount of analyte absorbed on the surface colloids. The analysis here is focusing on the shifting and the existence of the peaks. The resolution of the Raman system is 5 $cm^{-1}$, so only a $\Delta$ shift that is greater than 5 $cm^{-1}$ can be considered as reliable analysis. As literature outlines, cisplatin has a highly favorable binding specificity to guanine at the N7 position[25], which can be observed at 960 $cm^{-1}$. Observations suggest no shift and peak disappearance when the ratio of DNA bases to drugs is 5:1 and the sample is incubated for 24 hours. However, when the ratio was changed to 1:1, there is a red shift at 870 → 864 $cm^{-1}$ and blue shift at 1196 → 1205 $cm^{-1}$. The carbonyl-stretching band is at 1690 $cm^{-1}$. The red shifts are observed in both ratios for 24 hours, 1690 → 1676 $cm^{-1}$ and 1690 → 1664 $cm^{-1}$, but after 48 hours, they do not show any shift. This redshift marks that an interligand hydrogen bond is formed between the carbonyl group and the ammine ligand of cisplatin[39]. The binding of cisplatin to N7 of guanine is the hydrogen bonding between

the carbonyl oxygen (C6) and the hydrogen of the ammonia ligand. The SERS bands at 1440 cm $^{-1}$ shift upon platination and all four lines are indicated by $NH_2$ scissoring.

**SERS OF CARBOPLATIN MODIFICATION TO GUANINE**

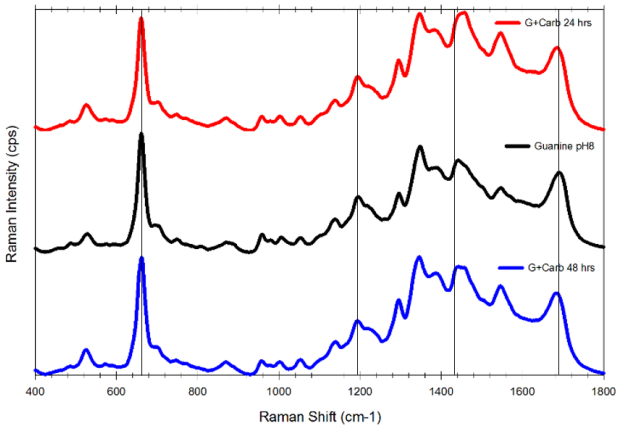


Figure 10. Surface-enhanced Raman spectrum of guanine was obtained at pH 8 (black), after incubation with carboplatin (5:1 ratio) for 24 hours (red) and 48 hours (blue); excitation laser, 780 nm; exposure time, 3 s; guanine concentration, $10^{-4}$ M; carboplatin concentration $10^{-4}$ M.

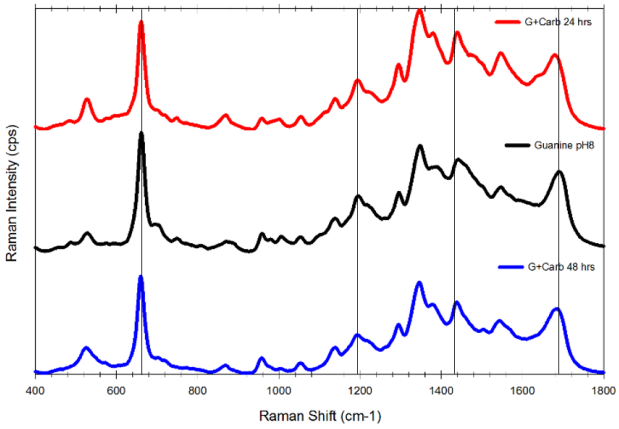


Figure 11. Surface-enhanced Raman spectrum of guanine was obtained at pH 8 (black), after incubation with carboplatin (1:1 ratio) for 24 hours (red) and 48 hours (blue); excitation laser, 780 nm; exposure time, 3 s; guanine concentration, $10^{-4}$ M; carboplatin concentration $10^{-4}$ M.

**Table 5. Raman Shift Values from SERS Spectra of Guanine at pH 8 and after incubation with carboplatin (5:1 ratio) within 5 $cm^{-1}$ resolutions and Assignment to Vibrations of the Guanine Molecule (Based on Reference 39).**

| Raman shift ($cm^{-1}$) | | | | | Assignments [39] |
|---|---|---|---|---|---|
| **Guanine** | **G+Carb 5:1 24hrs** | **Δ shift** | **G+Carb 5:1 48hrs** | **Δ shift** | |
| 527.91 | 525.37 | -2.54 | 524.40 | -3.51 | Deforming R6 (squeezing C6N1C2, N3C4C5), deforming R6 (squeezing C5C6N1, C2N3C4) |
| 660.97 | 660.36 | -0.61 | 661.32 | 0.35 | Breathing R6, wagging N1H |
| 870.21 | 869.60 | -0.61 | 869.60 | -0.61 | Def R5 (squeezing C4N9C8, stretching C5N7), R6 (squeezing N1C2N3) |
| 958.92 | 958.31 | -0.61 | 957.34 | -1.58 | Deforming R5 (squeezing N7C8N9), stretching PtN7 |
| 1053.42 | 1052.80 | -0.61 | 1053.77 | 0.35 | Rocking $NH_2$, C2N3-C6N1, bending N9H, C8H, stretching C8N9, stretching N1C2 |
| 1138.27 | 1138.62 | 0.35 | 1139.58 | 1.32 | Stretching C6N1-C4N9, rocking $NH_2$ |
| 1196.12 | 1194.55 | -1.58 | 1193.58 | -2.54 | Stretching PtN7 + C6N1 + C4N9, bending C8H, N9H, stretching C5N7, deforming R6 (squeezing N3C4C5) |
| 1295.44 | 1294.83 | -0.61 | 1294.83 | -0.61 | Bending N1H, stretching C5N7-C5C6-C2N10-N3C4, deforming $NH_3$ |
| 1348.47 | 1346.89 | -1.58 | 1345.93 | -2.54 | Stretching C5N7-C5C6 + C4N9 + C2N10(-N3C4), bending N1H, deforming $NH_3$ |
| 1388.01 | 1383.54 | -4.47 | 1386.43 | -1.58 | Stretching N1C2 + C4N9-C4C5(+N7C8), bending N1H, bending N9H, stretching C8N9-C5N7 |
| 1440.07 | 1456.82 | 16.74 | 1442.35 | 2.28 | Stretching N7C8 + N1C2-C4N9-C6O-C5C6, scissoring $NH_2$, bending C8H, N1H, stretching N7C8-N1C2 + C6O |
| 1547.10 | 1545.53 | -1.58 | 1545.53 | -1.58 | Scissoring $NH_2$, stretching C2N10-C2N3 |
| 1689.81 | 1685.34 | -4.47 | 1683.41 | -6.40 | Stretching C6O-C5C6, bending N1H, deforming $NH_3$ |

**Table 6. Raman Shift Values from SERS Spectra of Guanine at pH 8 and after incubation with carboplatin (1:1 ratio) within 5 $cm^{-1}$ resolutions and Assignment to Vibrations of the Guanine Molecule (Based on Reference 39).**

| Raman shift ($cm^{-1}$) | | | | | Assignments [39] |
|---|---|---|---|---|---|
| **Guanine** | **G+Carb 1:1 24hrs** | **Δ shift** | **G+Carb 1:1 48hrs** | **Δ shift** | |
| 527.91 | 526.33 | -1.58 | 525.37 | -2.54 | Deforming R6 (squeezing C6N1C2, N3C4C5), deforming R6 (squeezing C5C6N1, C2N3C4) |
| 660.97 | 660.36 | -0.61 | 659.40 | -1.58 | Breathing R6, wagging N1H |
| 870.21 | 869.60 | -0.61 | 868.63 | -1.58 | Def R5 (squeezing C4N9C8, stretching C5N7), R6 (squeezing N1C2N3) |
| 958.92 | 958.31 | -0.61 | 958.31 | -0.61 | Deforming R5 (squeezing N7C8N9), stretching PtN7 |
| 1053.42 | 1054.73 | 1.32 | 1053.77 | 0.35 | Rocking $NH_2$, C2N3-C6N1, bending N9H, C8H, stretching C8N9, stretching N1C2 |
| 1138.27 | 1138.62 | 0.35 | 1137.66 | -0.61 | Stretching C6N1-C4N9, rocking $NH_2$ |
| 1196.12 | 1193.58 | -2.54 | 1192.62 | -3.51 | Stretching PtN7 + C6N1 + C4N9, bending C8H, N9H, stretching C5N7, deforming R6 (squeezing N3C4C5) |
| 1295.44 | 1294.83 | -0.61 | 1294.83 | -0.61 | Bending N1H, stretching C5N7-C5C6-C2N10-N3C4, deforming $NH_3$ |
| 1348.47 | 1345.93 | -2.54 | 1345.93 | -2.54 | Stretching C5N7-C5C6 + C4N9 + C2N10(-N3C4), bending N1H, deforming $NH_3$ |
| 1388.01 | 1379.68 | -8.33 | 1377.75 | -10.26 | Stretching N1C2 + C4N9-C4C5(+N7C8), bending N1H, bending N9H, stretching C8N9-C5N7 |
| 1440.07 | 1439.46 | -0.61 | 1437.53 | -2.54 | Stretching N7C8 + N1C2-C4N9-C6O-C5C6, scissoring $NH_2$, bending C8H, N1H, stretching N7C8-N1C2 + C6O |
| 1547.10 | 1545.53 | -1.58 | 1543.60 | -3.51 | Scissoring $NH_2$, stretching C2N10-C2N3 |
| 1689.81 | 1679.55 | -10.26 | 1682.45 | -7.36 | Stretching C6O-C5C6, bending N1H, deforming $NH_3$ |

The SERS spectra of carboplatin and guanine complexes with different conditions such as ratio and incubation times were collected. Figure 10 shows the comparison between the SERS spectrum of guanine and the SERS spectrum of guanine upon adding carboplatin (5:1 ratio) for 24 hours and 48 hours. Table 5 gives the Raman shift and peak assignments of Figure 10. Figure 11 shows the comparison between the SERS spectrum of guanine and the SERS spectrum of guanine upon adding carboplatin (1:1 ratio) for 24 hours and 48 hours. Table 6 gives the Raman shift and peak assignments of Figure 11.

As seen in Figure 10 and Figure 11, the SERS spectra of carboplatin and guanine complexes show relative spectral changes, particularly in the region 400 – 1800 $cm^{-1}$. The distinct peak at 700 $cm^{-1}$, 750 $cm^{-1}$, and 1220 $cm^{-1}$ of red and blue lines seem to have fewer enhancements and are likely to disappear. The peaks show up at 750 $cm^{-1}$ when the ratio of DNA bases to carboplatin is 5:1, but the peaks do not show up when the addition of carboplatin is 5 fold higher. Similar to cisplatin, carboplatin also favors to bind to guanine at the N7 position, which can be observed at 960 $cm^{-1}$. However, no changes or shifts are observed in this position in both ratio and incubation time. $\Delta$ shifts that are greater than 5 $cm^{-1}$ in 5:1 ratios are 1385 $cm^{-1}$, 1440 $cm^{-1}$ and 1685 $cm^{-1}$ for 24 hours. This means there is a stretching at carbonyl oxygen C6O, bending at N1H, and scissoring at $NH_2$, while the peak at 1440 $cm^{-1}$ does not show change for 48 hours. When the ratio was changed to 1:1, the $\Delta$ shifts that are greater than 5 $cm^{-1}$ are observed at 1385 $cm^{-1}$ and 1685 $cm^{-1}$ for 24 hours and 48 hours.

**SERS OF CISPLATIN MODIFICATION TO GUANINE WHEN DRUG DOSAGE IS INCREASED**

An investigation of cisplatin modification to guanine with drug high-dose strategy was developed. In order to make SERS of cisplatin modification to guanine samples, $10^{-5}$ M of guanine and $10^{-4}$ M of cisplatin were used. The stock solutions were recorded at pH 9. Two sets

of samples were prepared as 5:1 and 1:1 guanine to cisplatin volume ratio. These two sample vials were incubated in a water bath for 5 hours. Then, the samples were combined with silver nanoparticle 0.2 M of $MgSO_4$. The scans were collected 12 hours after the incubation period. As calculated, the final molar ratio of the first sample (5:1) was 1:2 guanine to cisplatin and the second sample (1:1) was 1:10 guanine to cisplatin. SERS spectra of guanine complexes with cisplatin at different volume ratios are shown in Figure 12. The shift assignments for the Raman bands are indicated in Table 7.

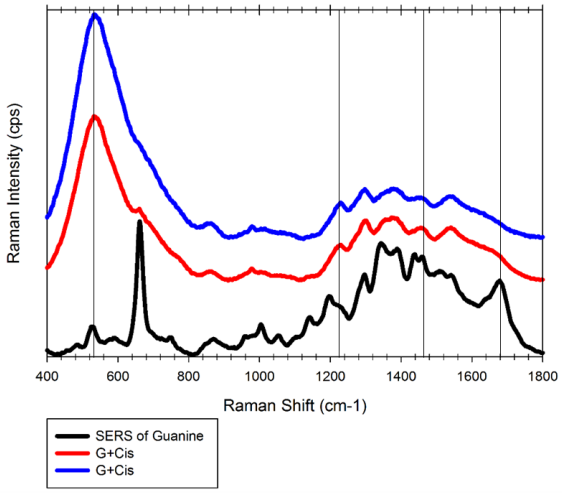


Figure 12. Surface-enhanced Raman spectrum of $10^{-5}$ M guanine was obtained at pH 9 (black), after incubation with cisplatin 1:2 ratio (red) and 1:10 ratio (blue); excitation laser, 780 nm; exposure time, 3 s; guanine concentration, $10^{-5}$ M; cisplatin concentration $10^{-4}$ M.

**Table 7. Raman Shift Values from SERS Spectra of Guanine at pH 9 and after incubation with cisplatin 1:2 ratio and 1:10 ratio within 5 $cm^{-1}$ resolutions and Assignment to Vibrations of the Guanine Molecule (Based on Reference 39).**

| Raman shift ($cm^{-1}$) | | | | | Assignments [39] |
|---|---|---|---|---|---|
| **Guanine** | **G+Cis (1:2)** | **Δ shift** | **G+Cis (1:10)** | **Δ shift** | |
| 525.58 | 532.67 | 7.09 | 533.17 | 7.59 | Deforming R6 (squeezing C6N1C2, N3C4C5), deforming R6 (squeeze C5C6N1, C2N3C4) |
| 661.7 | N/A | N/A | N/A | N/A | Breathing R6, wagging N1H |
| 870.48 | 870.48 | 0 | 870.48 | 0 | Deforming R5 (squeezing C4N9C8, stretching C5N7), R6 (squeezing N1C2N3) |
| 1052.75 | N/A | N/A | N/A | N/A | Rocking $NH_2$, C2N3-C6N1, bending N9H, C8H, stretching C8N9, stretching N1C2 |
| 1142.53 | N/A | N/A | N/A | N/A | Stretching C6N1-C4N9, rocking $NH_2$ |
| 1196.3 | 1231 | 34.7 | 1229.2 | 32.9 | Stretching PtN7 + C6N1 + C4N9, bending C8H, N9H, stretching C5N7, deforming R6 (squeezing N3C4C5) |
| 1296.85 | 1300.32 | 3.47 | 1297.61 | 0.76 | Bending N1H, stretching C5N7-C5C6-C2N10-N3C4, deforming $NH_3$ |
| 1343.28 | 1355.5 | 12.22 | N/A | N/A | Stretching C5N7-C5C6 + C4N9 + C2N10(-N3C4), bending N1H, deforming $NH_3$ |
| 1388.82 | 1373.23 | -15.59 | 1378.74 | -10.08 | Stretching N1C2 + C4N9-C4C5(+N7C8), bending N1H, bending N9H, stretching C8N9-C5N7 |
| 1438.52 | 1461.6 | 23.08 | 1458.7 | 20.18 | Stretching N7C8 + N1C2-C4N9-C6O-C5C6, scissoring $NH_2$, bending C8H, N1H, stretching N7C8-N1C2 + C6O |
| N/A | 1540.79 | N/A | 1545.45 | N/A | Scissoring $NH_2$, stretching C2N10-C2N3 |
| 1678.44 | N/A | N/A | N/A | N/A | Stretching C6O-C5C6, bending N1H, deforming $NH_3$ |

In the first sample, when guanine – cisplatin complexes compares to guanine only, the distinct peaks at 660 $cm^{-1}$, 1053 $cm^{-1}$, 1143 $cm^{-1}$, 1540 $cm^{-1}$, and 1678 $cm^{-1}$ disappear. A majority of the rest show relative red shifts at 525 $cm^{-1}$, 1196 $cm^{-1}$, 1343 $cm^{-1}$, and 1438 $cm^{-1}$. The peak at 1388 $cm^{-1}$ shows the blue shift to 1373 $cm^{-1}$.

In the second sample, the peak at 660 $cm^{-1}$, 1053 $cm^{-1}$, 1143 $cm^{-1}$, 1343 $cm^{-1}$, 1540 $cm^{-1}$, and 1678 $cm^{-1}$ are missing when cisplatin was added to guanine. The rest of the peaks, 525 $cm^{-1}$, 1196 $cm^{-1}$, 1343 $cm^{-1}$, and 1438 $cm^{-1}$ are showing large shifts compared to guanine only. When the second sample compares to the first sample, the peaks at 525 $cm^{-1}$ and 1388 $cm^{-1}$ are shifted to a longer wavenumber, while the peaks at 1196 $cm^{-1}$, 1296 $cm^{-1}$, and 1438 $cm^{-1}$ are shifted to a shorter wavenumber.

**CONCLUSION**

The study of how platinum-based drugs modify guanine is intensive work because the modifications are all dependent on pH, ratio, concentration, and incubation time. Cisplatin and carboplatin alter the structure of guanine at the molecular level. The interaction of platinum drugs and guanine was revealed at pH 8. Numerous experiments and analysis showed that guanine is most sensitive to the binding of platinum drugs when guanine to cisplatin was 5:1 or guanine to carboplatin was 1:1, $10^{-4}$ M of guanine. The reaction took place during the first 24 hours. After 24 hours, the bases started to degrade. The examinations also displayed that cisplatin was more effective in binding to guanine than carboplatin because most of conformational changes appeared in the cisplatin-guanine complex spectrum. The high dose of cisplatin experiments exposed the most obvious changes comparing to the low dose of drugs experiments. The cisplatin was 2 fold or 10 fold higher than guanine, so it damaged the bases and the spectra in the high dose experiment did not show the significant peaks in the spectral range, 400 → 1800 $cm^{-1}$.

In the near future, the study of adenine upon the presence of cisplatin or carboplatin should be completed complimentary to this study. From that, there will be more explanation to why platinum-based drugs prefer to bind to guanine over adenine[25]. Additionally, the modification of platinum drugs on selective DNA sequences should be investigated to fully explore the binding behaviors of platinum drugs to DNA.

# CHAPTER VI

# NEW COPPER COMPLEXES INTERACTED WITH DNA FOR THEIR POTENTIAL USE AS ANTICANCER AGENTS

## OVERVIEW

The discovery of cisplatin in the 1960s and the introduction into clinical trial in the 1970s has stimulated the research of metal-based drugs[6]. Numerous cisplatin derivatives have been developed and presented with the improvement on side effects and broad spectrum of activity such as carboplatin, nedaplatin, oxaliplatin, or lobaplatin. Recently, many metal-based compounds have been synthesized and found to be anticancer agents such as ruthenium (Ru (II), Ru (III)), gold (Au (I), Au (III)), and titanium (Ti (IV))[40]. In the preceding chapter, the structures and mechanisms of platinum-based drugs, cisplatin, and carboplatin have been discussed. This chapter will cover the new copper compounds that might have anticancer properties. Copper-based complexes have displayed possible usage as antimicrobial, antiviral, anti-inflammatory, and antitumor agents, and enzyme inhibitors, or chemcial nucleases[18]. Copper-based complexes have been chosen to investigate, because they may be less toxic than platinum-based drugs[14,18].

Benzimidazole-based copper complexes are found to inhibit the tumor cells' growth. These complexes can induce apotosis of HCT116 cells by damaging the DNA, dysfuncting the mitrochondrion, and producing reactive oxygen species[41]. The copper complexes containing novel Schiff base of Quinoline-2 Carboxaldehydes are efficient in antiprofilerative and proapoptotic activity in PC-3 and LNCaP prostate cancer cells[42]. Thiosemicarbazone Cu(II) complex has proven to inhibit the growth of HeLa cells. It is suggested that this complex can cause DNA fragmentation and oxidative DNA damage[43].

The properties of copper-based complexes are decided by the nature of ligands 14. In this chapter, the copper complexes will be incorporated with 1,10-phenanthroline, a heteroatomic molecule. It has been used in synthesis with many metal complexes due to its properties, for example, rigidity, aromaticity, basicity, and chelating capability[44]. 1,10-phenanthroline has acted as an important ligand that exhibits chemical nuclease activity like $Cu(phen)_2$[45]. It also binds and leads to DNA damage through minor-groove binding[45].

**MATERIALS AND STRUCTURE OF COPPER COMPLEXES**

Mikaela Wilk carried out the synthesis of new copper complexes in Dr. Omary's lab. The starting materials for the synthesis were Tetrakis(acetonitrile)copper(I) tetrafluoroborate and 1,10-phenanthroline. The structure of newly synthesized copper complexes is presented in Figures 14, 15, 16, and 17.


Figure 13. Structure for Tetrakis(acetonitrile)copper(I) tetrafluoroborate, $Cu(MeCN)_4BF_4$ (left) and 1,10-phenanthroline, $C_{12}H_8N_2$ (right).

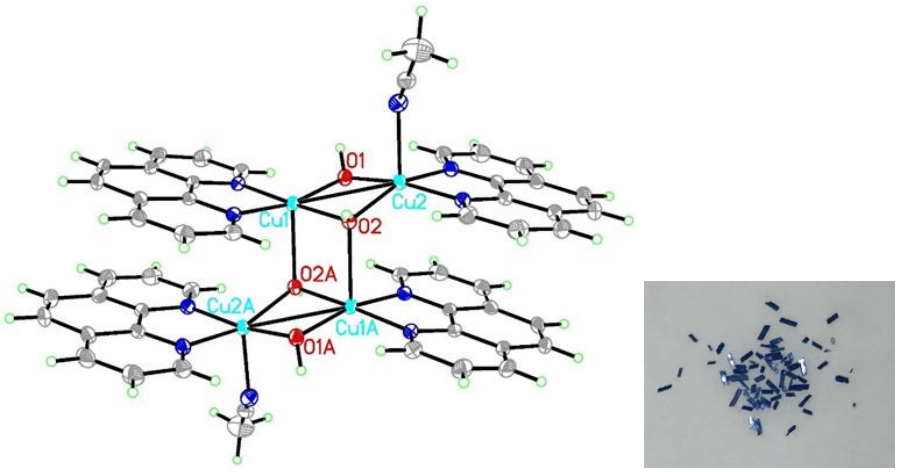


Figure 14. Structure and atom labeling for $[Cu_4(phen)_4(CH_3CN)_2(OH)_4]_4^+(BF_4^-)_4$/ blue color.

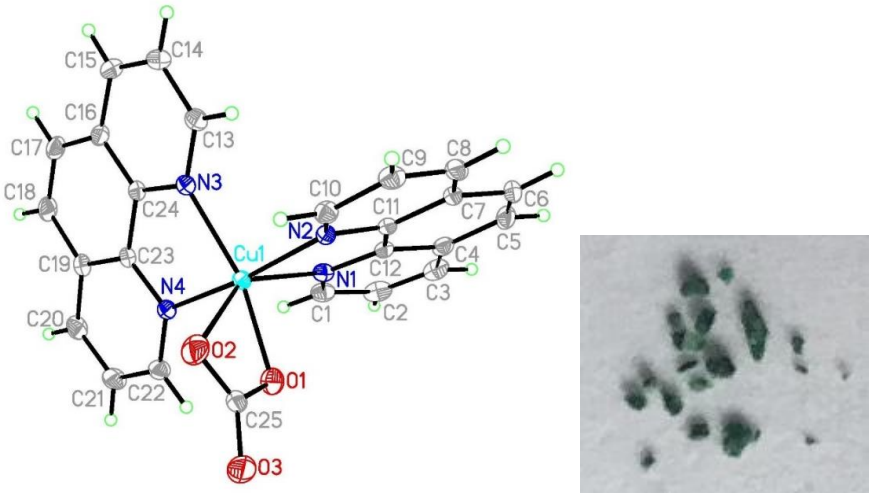


Figure 15. Structure and atom labeling for $Cu(phen)_2CO_3(H_2O)_7$/ green (1) color.

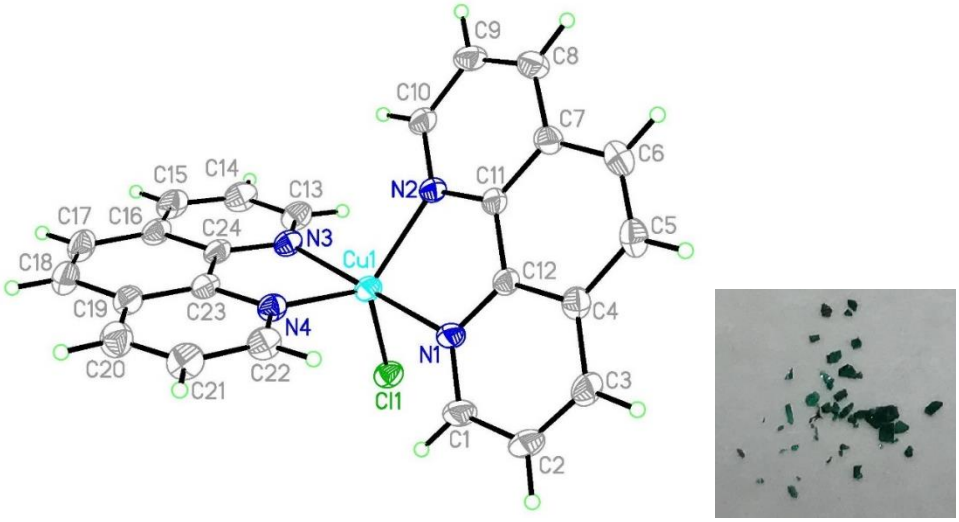


Figure 16. Structure and atom labeling for $[Cu(phen)_2Cl]^+BF_4^-$/ green (2) color.

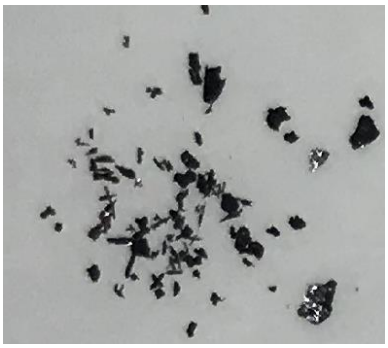

Figure 17. Picture of $Cu(phen)_n$/ black color.

**EXPERIMENTAL**

IR, normal Raman, and SERS were employed to study four new copper complexes: $[Cu_4(phen)_4(CH_3CN)_2(OH)_4]_4^+(BF_4^-)_4$/ blue color, $Cu(phen)_2CO_3(H_2O)_7$/ green (1) color, $[Cu(phen)_2Cl]^+BF_4^-$/ green (2) color, and $Cu(phen)_n$/ black color. This study is an important step to comprehend the characteristics of the complexes prior to studying the behaviors of these copper complexes with DNA bases. The samples of normal Raman and IR studies were completed in the crystalline form. In the normal Raman experiment, the copper crystals were placed between a quartz glass and a cover glass. Then, the glass was transferred to the Raman system to do the scans. In the IR experiment, the copper crystals were placed on the ATR diamond, and then the scans were collected. Contrarily, the SERS experiment was involved in the liquid form. Grams of different copper crystals were dissolved in 1 mL ultra-pure water to the final concentration of $10^{-3}$ M as follows:

- $1.56x10^{-3}$ g of solid $[Cu_4(phen)_4(CH_3CN)_2(OH)_4]_4^+(BF_4^-)_4$/ blue color.
- $6.10x10^{-4}$ g of solid $Cu(phen)_2CO_3(H_2O)_7$/ green (1) color.
- $5.65x10^{-4}$ g of solid $[Cu(phen)_2Cl]^+BF_4^-$/ green (2) color.
- $1.70x10^{-3}$ g of solid $Cu(phen)_n$/ black color.

100 μL of each solution was transferred to four different vials. 800 μL of silver nanoparticles were added along with 100 μL of 0.2 M of $MgSO_4$. After a period of time, all samples were aggregated, and then they were analyzed through Raman scattering. The IR, normal Raman, and SERS spectra are presented in the graphs below.

## IR, RAMAN, AND SERS OF COPPER COMPLEXES

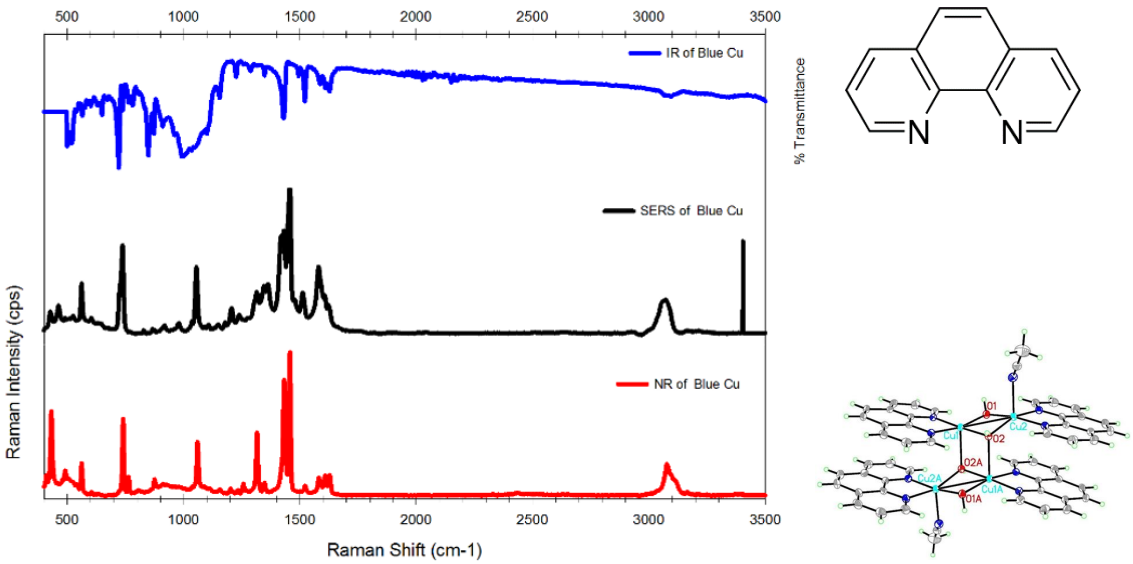


Figure 18. Fourier-transform infrared (blue), surface-enhanced Raman (black), and normal Raman (red) spectra of $[Cu_4(phen)_4(CH_3CN)_2(OH)_4]_4^+(BF_4^-)_4$/ blue color.

**Table 8. Expected and Observed IR Frequencies and Functional Group Assignment for $[Cu_4(phen)_4(CH_3CN)_2(OH)_4]_4^+(BF_4^-)_4$/ Blue Color.**

| Functional Group | Expected Frequency Range ($cm^{-1}$) | Observed Frequencies ($cm^{-1}$) |
|---|---|---|
| C-H Alkanes | 2850-3000 | N/A |
| | 1340-1470 | 1348 |
| C-H Aromatic rings | 3010-3100 | 3095 |
| | 690-900 | 721, 738, 764, 782, 848, 872, 910 |
| C=C Aromatic rings | 1450-1600 | 1430, 1495, 1522, 1587, 1627 |
| C-N Aromatic Amine | 1266-1342 | 1226, 1288, 1348 |
| O-H (free) | 3590-3650 | 3628 |
| O-H (H-bonded) | 3100-3600 | 3330, 3564 |
| C≡N Nitriles | 2200-2400 | N/A |
| $BF_4^-$ | 1050-1100 | 993 |
| Cu-N | ~350-450 | 423, 470 |
| N-Cu-N | ~200-300 | 307 |

Blue copper complex has the chemical structures $[Cu_4(phen)_4(CH_3CN)_2(OH)_4]_4^+(BF_4^-)_4$. Figure 18 illustrates the relationship of vibrational motion between IR, normal Raman, and SERS and Table 8 shows the IR frequencies. The IR and normal Raman of

$[Cu_4(phen)_4(CH_3CN)_2(OH)_4]_4^+(BF_4^-)_4$/ blue color share similarities between two spectra. There are two peaks, 750 $cm^{-1}$ and 1450 $cm^{-1}$, that are observed in both IR and normal Raman. The SERS spectrum shows six peaks, 450 $cm^{-1}$, 580 $cm^{-1}$, 750 $cm^{-1}$, 1150 $cm^{-1}$, 1300 $cm^{-1}$, and 1450 $cm^{-1}$, which are visible in the normal Raman spectrum. The peak at 1520 $cm^{-1}$ and 1580 $cm^{-1}$ are enhanced to clear visibility in the SERS spectrum. The line at 3400 $cm^{-1}$ has not been observed in normal Raman. The Cu-N bindings are found at 423 and 470 $cm^{-1}$.

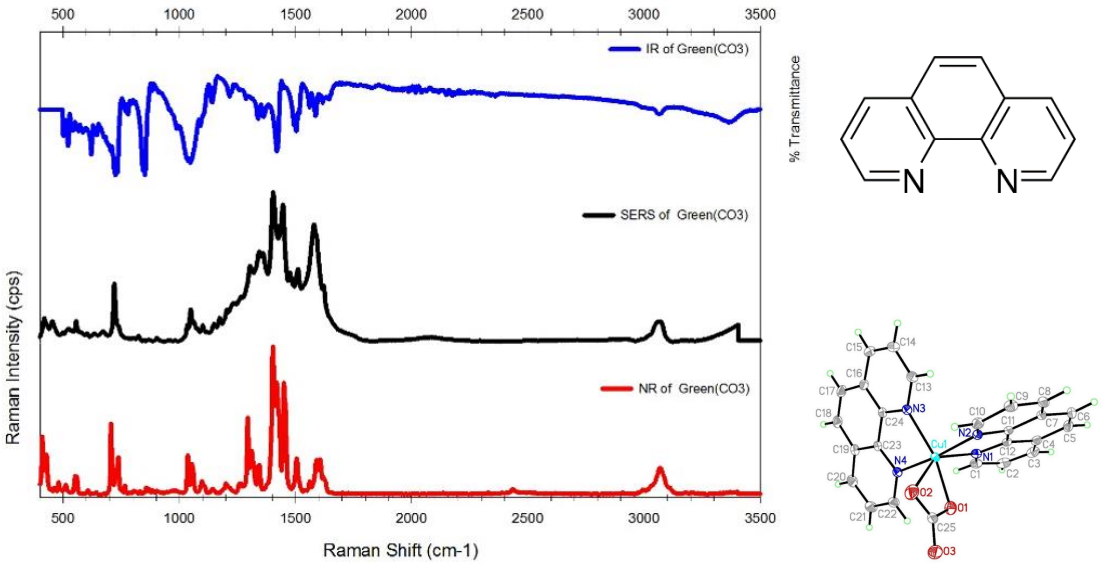


Figure 19. Fourier-transform infrared (blue), surface-enhanced Raman (black), and normal Raman (red) spectra of $Cu(phen)_2CO_3(H_2O)_7$/ green (1) color.

**Table 9. Expected and Observed IR Frequencies and Functional Group Assignment for $Cu(phen)_2CO_3(H_2O)_7$/ Green (1) Color.**

| Functional Group | Expected Frequency Range ($cm^{-1}$) | Observed Frequencies ($cm^{-1}$) |
|---|---|---|
| C-H Aromatic rings | 3010-3100 | 3064 |
| | 690-900 | 705, 725, 769, 843 |
| C=C Aromatic rings | 1450-1600 | 1419, 1494, 1503, 1560, 1586, 1616 |
| C-N Aromatic Amine | 1266-1342 | 1338 |
| O-H (H-bonded) | 3100-3600 | 3364 |
| Covalent carbonate | 1225-1325 | 1225, 1328 |
| | 990-1090 | 1048 |
| Cu-N | ~350-450 | 419 |
| N-Cu-N | ~200-300 | 248 |

Green (1) copper complex has the chemical structure $Cu(phen)_2CO_3(H_2O)_7$. Table 9 shows the IR frequencies. In Figure 19, the IR spectrum shows one peak at 850 $cm^{-1}$ that are not seen in the normal Raman. The peaks at 700 $cm^{-1}$, 1050 $cm^{-1}$, 1400 $cm^{-1}$, 1500 $cm^{-1}$, and 1600 $cm^{-1}$ are shown in both normal Raman and IR. The SERS and normal Raman of $Cu(phen)_2CO_3(H_2O)_7$/ green (1) color show similarities, except one peak at 1300 $cm^{-1}$. This peak is clearly resolved in normal Raman, but weakly visible in the SERS spectrum. There is a peak at 3400 $cm^{-1}$ as seen in the SERS. The Cu-N bindings are observed at 419 and 248 $cm^{-1}$.

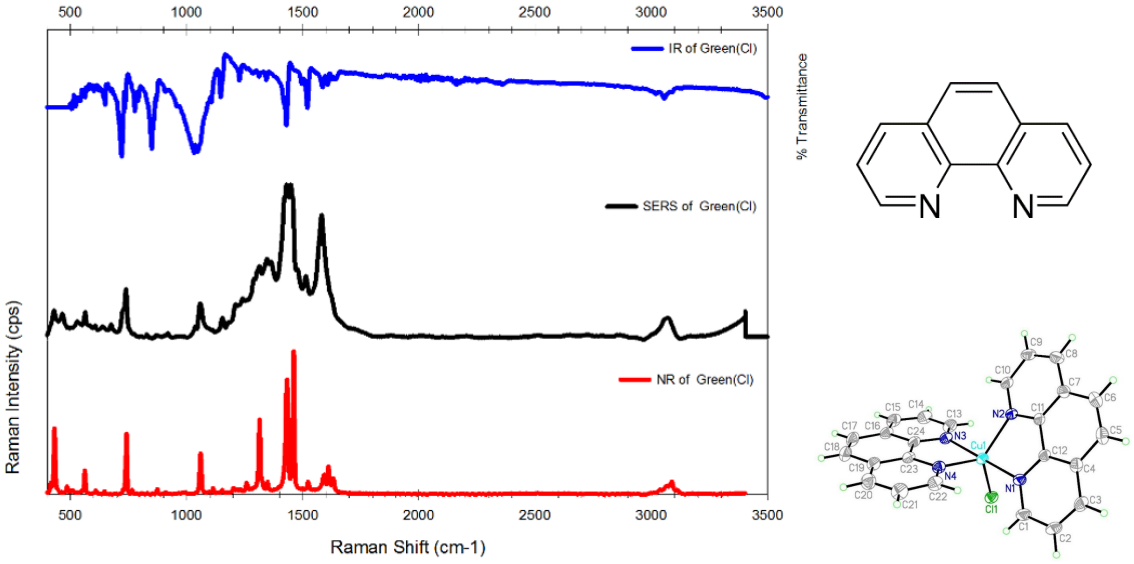


Figure 20. Fourier-transform infrared (blue), surface-enhanced Raman (black), and normal Raman (red) spectra of $[Cu(phen)_2Cl]^+BF_4^-$/ green (2) color.

**Table 10. Expected and Observed IR Frequencies and Functional Group Assignment for $[Cu(phen)_2Cl]^+BF_4^-$/ Green (2) Color.**

| Functional Group | Expected Frequency Range ($cm^{-1}$) | Observed Frequencies ($cm^{-1}$) |
|---|---|---|
| C-H Aromatic rings | 3010-3100 | 3020, 3055 |
| | 690-900 | 721, 778, 791, 851, 910 |
| C=C Aromatic rings | 1450-1600 | 1417, 1429, 1495, 1520, 1585, 1606, 1626, 1641 |
| C-N Aromatic Amine | 1266-1342 | 1227, 1282, 1311, 1343 |
| O-H (H-bonded) | 3100-3600 | 3493, 3581 |
| $BF_4^-$ | 1050-1100 | 1032, 1048, 1107 |
| Cu-N | ~350-450 | 435 |
| N-Cu-N | ~200-300 | 278 |

Green (2) copper complex has the chemical structure $[Cu(phen)_2Cl]^+BF_4^-$. Table 10 shows the IR frequencies. In Figure 20, there is a peak at 850 $cm^{-1}$, that is seen in the IR spectrum but not in normal Raman. Several peaks are common in both IR and normal Raman of $[Cu(phen)_2Cl]^+BF_4^-$/ green (2) color, such as 700 $cm^{-1}$, 1050 $cm^{-1}$, and 1450 $cm^{-1}$. Two peaks at 550 $cm^{-1}$ and 1350 $cm^{-1}$ appear in normal Raman, not in IR. The peak that is at 1450 $cm^{-1}$, looks like double peaks. The SERS and normal Raman spectra of $[Cu(phen)_2Cl]^+BF_4^-$/ green (2) color are not very similar. Three peaks are seen in both SERS and normal Raman spectra that are 750 $cm^{-1}$, 1050 $cm^{-1}$, and 1450 $cm^{-1}$. A cluster of peaks is shown between 1200 $cm^{-1}$ and 1400 $cm^{-1}$. The peak at 1600 $cm^{-1}$ is enhanced in the SERS spectrum. The peak at 3400 $cm^{-1}$ is not seen in the normal Raman spectrum. The complex of $[Cu(phen)_2Cl]^+BF_4^-$ does not hold any water in its structure, but the IR, SERS, and Raman spectra all show a pump in the region 3000 – 3500 $cm^{-1}$. The complex could absorb water from the air. The Cu-N bindings are found at 435 and 278 $cm^{-1}$.

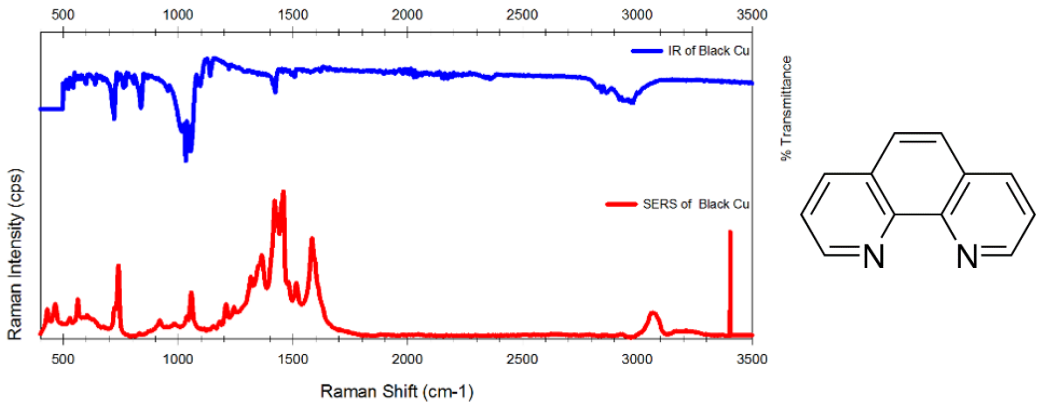


Figure 21. Fourier-transform infrared (blue), surface-enhanced Raman (red) spectra of $Cu(phen)_n$/ black color.

**Table 11. Expected and Observed IR Frequencies and Functional Group Assignment for $Cu(phen)_n$/ Black Color.**

| Functional Group | Expected Frequency Range ($cm^{-1}$) | Observed Frequencies ($cm^{-1}$) |
|---|---|---|
| C-H Aromatic rings | 3010-3100 | 3070 |
| | 690-900 | 721, 762, 770, 838, 868 |
| C=C Aromatic rings | 1450-1600 | 1414, 1423, 1446, 1495, 1508, 1589, 1622 |
| C-N Aromatic Amine | 1266-1342 | 1221, 1288, 1340 |
| $BF_4^-$ | 1050-1100 | 1054, 1095 |
| Cu-N | ~350-450 | 435 |
| N-Cu-N | ~200-300 | N/A |

Black copper complex has the general chemical formula of $Cu(phen)_n$. Figure 21 presents the IR and SERS of $Cu(phen)_n$/ black color. The IR frequencies can be found in table 11. The chemical structure of $Cu(phen)_n$/ black color had not been performed. Only the IR and SERS readings of $Cu(phen)_n$/ black color could be obtained. Normal Raman could not be obtained because the sample was decomposed when the laser hit. Comparing the IR and SERS interpretation of $Cu(phen)_n$/ black color, two peaks are seen at 750 $cm^{-1}$ and 1050 $cm^{-1}$ in both. Some other peaks are detected in SERS such as 550 $cm^{-1}$, 750 $cm^{-1}$, 1350 $cm^{-1}$, 1450 $cm^{-1}$,1600 $cm^{-1}$, and 3400 $cm^{-1}$. The Cu-N binding is detected at 435 $cm^{-1}$.

**CONCLUSION**

The IR, Raman, and SERS spectra of four newly synthesized copper complexes were analyzed and reported in this paper. The results indicated that the SERS spectra and Raman spectra give information about Cu-N bindings, while IR spectra does not. This is because the IR region is above 500 $cm^{-1}$. The complex of $[Cu_4(phen)_4(CH_3CN)_2(OH)_4]_4^+(BF_4^-)_4$/ blue color has OH group in its structure and the frequencies at 3330, 3564, and 3628 $cm^{-1}$ determine the presence of this functional group. The complex of $Cu(phen)_2CO_3(H_2O)_7$/ green (1) color has carbonate group and IR bands at 1225 and 1328 $cm^{-1}$. The complex of $[Cu(phen)_2Cl]^+BF_4^-$/ green (2) color do not have OH group in its structure, but the peak of absorbed water is found in the

region 3000 – 3500 $cm^{-1}$. The background signals and noise peaks were seen in SERS spectra instead of resolved peaks in the region 1200 – 1600 $cm^{-1}$. $Cu(phen)_n$/ black color only gave the SERS spectrum, while the normal Raman spectrum could not collect. The UV-Vis of $Cu(phen)_n$/ black color should be performed to figure out the appropriate laser wavelength. The common IR functional groups for all copper complexes were C-H aromatic rings, C=C aromatic ring, and C-N aromatic amine. Theoretical calculations will have to be done in order to figure out the vibrational assignments and adsorption modes of the complexes. This project will help further studies such as the interaction of copper complexes and DNA.

CHAPTER VII

# SURFACE-ENHANCED RAMAN SPECTROSCOPIC STUDIES OF NEW COPPER COMPLEXES MODIFICATION TO GUANINE OR ADENINE

## OVERVIEW

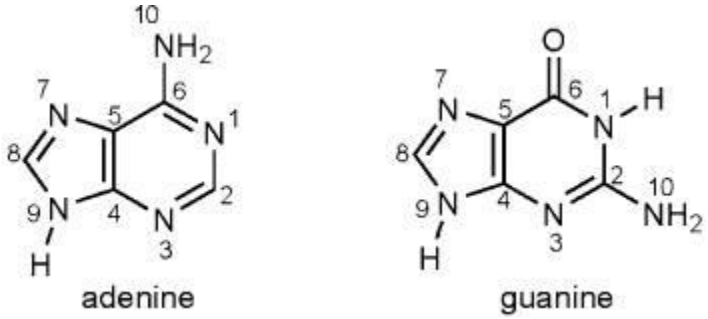


Figure 22. Structure and atom labeling for adenine and guanine[46].

Guanine (Molecular formula: $C_5H_5N_5O$) and adenine (Molecular formula: $C_5H_5N_5$) are both purine bases, which consist of a pyrimidine ring fused to an imidazole ring. Guanine has an amine group on C2 position and a carbonyl group on C6 position, while adenine has an amine group on C6 position (see Figure 22). In the study of DNA-drug interactions, purine bases have exhibited the potential sites for the binding of drugs. The platinum drugs, such as cisplatin, have revealed the preferential binding to the N7 position of guanine or adenine[25]. Also, cisplatin prefers to bind to guanine over adenine[25]. $CuCl_2$-guanine complex has been reported to preferentially bind to guanine at the N7 position and create a crosslink to DNA[47]. In another report, copper complexes have been known to form crosslinks with adenine at N9, N7, N3 and the bridging modes μ-N3,N7; μ-N7,N9; and μ-N1,N9[48]. Hence, the binding behaviors of copper complexes would be observed on both guanine and adenine. In the first stage of the copper anticancer agents study, SERS readings of guanine and adenine were collected. In the second stage, the modification of new copper complexes to guanine and adenine were investigated.

**EXPERIMENTAL**

The interactions between DNA bases and newly synthesized copper complexes were studied through the practice of the SERS technique. The study began with taking the scan on the guanine or adenine sample. This was an extra step that would help for further analysis before the interaction of four different copper compounds with guanine or adenine was examined. There is no documented data of copper complexes and DNA bases, so the sole purpose of this experiment is to establish the baseline of sample conditions for future SERS studies. The rough estimate of the final concentration for the samples was $10^{-3}$ M. This concentration was chosen because all four copper complexes were soluble at this maximum concentration. SERS samples also require the use of nanoparticles and salt. $MgSO_4$ was used to help for aggregation.

The procedure started by making the stock solution. Two stock solutions were produced as follows:

- Guanine stock solution: $1.51x10^{-4}$ g of solid guanine was dissolved in ultra-pure water to the concentration of $10^{-3}$ M.
- Adenine stock solution: $1.35x10^{-4}$ g of solid adenine was dissolved in ultra-pure water to the concentration of $10^{-3}$ M.

Then, 100 μL of stock solution was transferred to each vial and combined with silver nanoparticles and 0.2 M of $MgSO_4$. The final volume would be 1000 μL. Two base vials sat for two hours and the SERS spectra data was collected. In other vials, the solid copper complexes were added to base stock solutions. A total of eight samples were made as following:

- $1.56x10^{-3}$ g of solid $[Cu_4(phen)_4(CH_3CN)_2(OH)_4]_4^+(BF_4^-)_4$/ blue color to 1 mL of $10^{-3}$ M guanine or adenine stock solution.
- $6.10x10^{-4}$ g of solid $Cu(phen)_2CO_3(H_2O)_7$/ green (1) color to 1 mL of $10^{-3}$ M guanine or adenine stock solution.

- $5.65x10^{-4}$ g of solid $[Cu(phen)_2Cl]^+BF_4^-$/ green (2) color to 1 mL of $10^{-3}$ M guanine or adenine stock solution.
- $1.70x10^{-3}$ g of solid $Cu(phen)_n$/ black color to 1mL of $10^{-3}$ M guanine or adenine stock solution.

Next, 100 µL of eight different samples were transferred to eight different vials. The pH among vials was range 8 – 9. These vials were incubated in a water bath at 37°C for 24 hours. After the incubation period, the samples were removed from the water bath and they were added to silver nanoparticles and salt. The amount of silver nanoparticles was 800 µL, and salt was 100 µL. Once all samples were well aggregated, they were moved to the next step of taking SERS scans. The collected data has been revealed in the graphs below. The SERS spectra of copper complexes and the SERS spectra of DNA bases were added physically together. These new added spectra were plotted and aligned with collected SERS spectra of experimental addition.

**SERS OF GUANINE AND ADENINE**

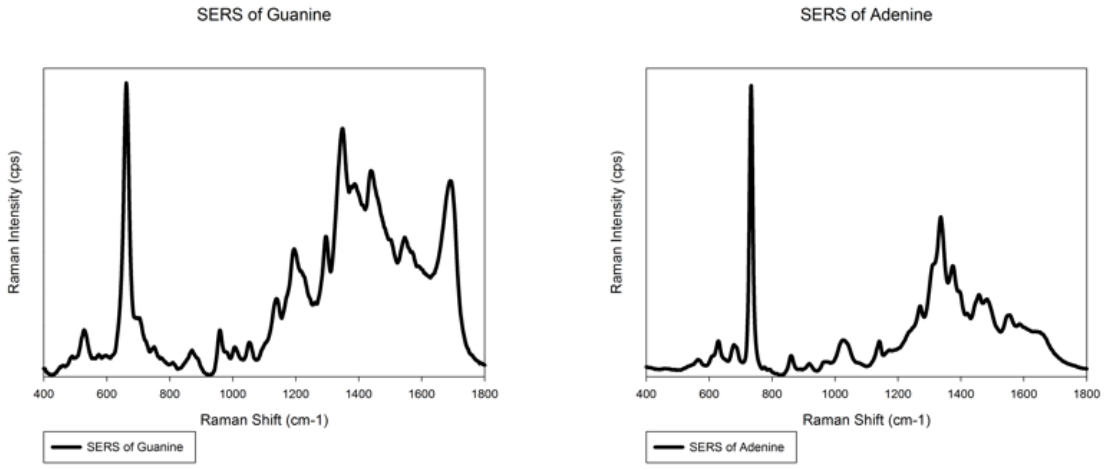


Figure 23. Surface-enhanced Raman spectra of guanine (left) and adenine (right); excitation laser, 780 nm; exposure time, 3 s; guanine concentration, $10^{-3}$ M.

**Table 12. Raman Shift Values from SERS Spectra of Guanine and Assignment to Vibrations of the Guanine Molecule (Based on Reference 46).**

| SERS of Guanine | |
|---|---|
| **Raman shift ($cm^{-1}$)** | **Assignments** [46] |
| 528.23 | 6-ring deforming |
| 662.06 | 6-ring breathing, 5-ring deforming, wagging $NH_2$ |
| 870.71 | 5-ring deforming, 6-ring deforming, wagging N9-H, N1-H |
| 959.12 | 5-ring deforming |
| 1006.09 | rocking $NH_2$, ring stretching C-N |
| 1052.55 | stretching N1-C2, C2-N3 |
| 1139.08 | rocking $NH_2$, ring stretching C-N |
| 1195.19 | bending C8-H, stretching C5-N7, N7-C8 |
| 1296.05 | ring stretching C-N, C-C, bending C8-H, rocking $NH_2$ |
| 1348.73 | bending N1-H, N10-H12, stretching C2-N10 |
| 1439.37 | ring stretching C-N, bending C8-H, N1-H, N10-H |
| 1546.24 | ring stretching C-N, scissoring $NH_2$, bending N1-H |
| 1690.6 | stretching C6=O, C5-C6, bending N1-H, scissoring $NH_2$ |

**Table 13. Raman Shift Values from SERS Spectra of Adenine and Assignment to Vibrations of the Adenine Molecule (Based on Reference 46).**

| SERS of Adenine | |
|---|---|
| **Raman shift ($cm^{-1}$)** | **Assignments** [46] |
| 629.15 | 6-ring deforming |
| 678.82 | 5-ring deforming |
| 733.23 | ring breathing |
| 860.51 | 6-ring deforming |
| 1028.29 | rocking $NH_2$ |
| 1140.99 | stretching C8-N9, bending N9-H, C8-H |
| 1270.76 | bending C8-H, N9-H, stretching N7-C8 |
| 1336.05 | stretching C5-N7, N1-C2, C2-N3, C5-C6, bending C2/8-H |
| 1374.55 | bending C2-H, N9-H, stretching C8-N9, C4-N9 |
| 1457.66 | stretching C2-N3, N1-C6, bending C2-H, scissoring $NH_2$ |
| 1555.37 | scissoring $NH_2$ |

In Figure 23, the SERS scans of guanine and adenine are shown. The assignments of SERS spectra are summarized on Tables 12 and 13. In the SERS spectra of guanine, 6-ring deformations were observed at 528 $cm^{-1}$ and 871 $cm^{-1}$, which can be observed at 629 $cm^{-1}$ and

861 $cm^{-1}$ in adenine. 5-ring deformations were observed at 662 $cm^{-1}$ and 959 $cm^{-1}$ in guanine and only at 679 $cm^{-1}$ in adenine. Ring breathings were observed in guanine and adenine at 662 $cm^{-1}$ and 733 $cm^{-1}$, respectively.

**COMPARISON BETWEEN ADDING TWO SPECTRA WITH EXPERIMENTAL ADDITIONS**

The comparison between adding two SERS spectra and experimental additions could help us to find out if new copper complexes can modify guanine or adenine. If there are similarities between two spectra, it means that the copper complexes do not bind to guanine or adenine. They will just stay as two separate molecules in the samples. If there are differences between two spectra, it could suggest that interactions are occurring between the copper complexes and guanine or adenine.

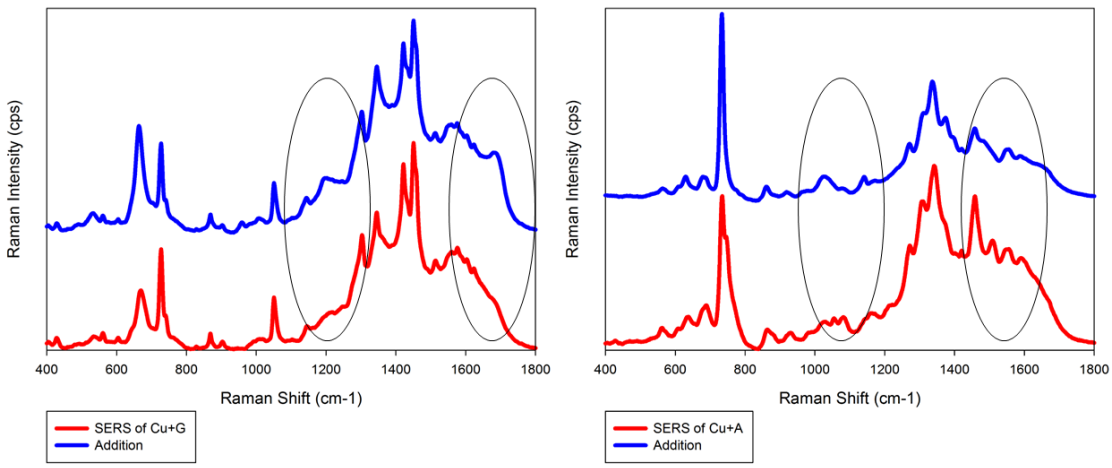


Figure 24. Surface-enhanced Raman spectra of $[Cu_4(phen)_4(CH_3CN)_2(OH)_4]_4^+(BF_4^-)_4$/ blue color with guanine (left) or adenine (right) by experimental addition (red) and adding two spectra (blue).

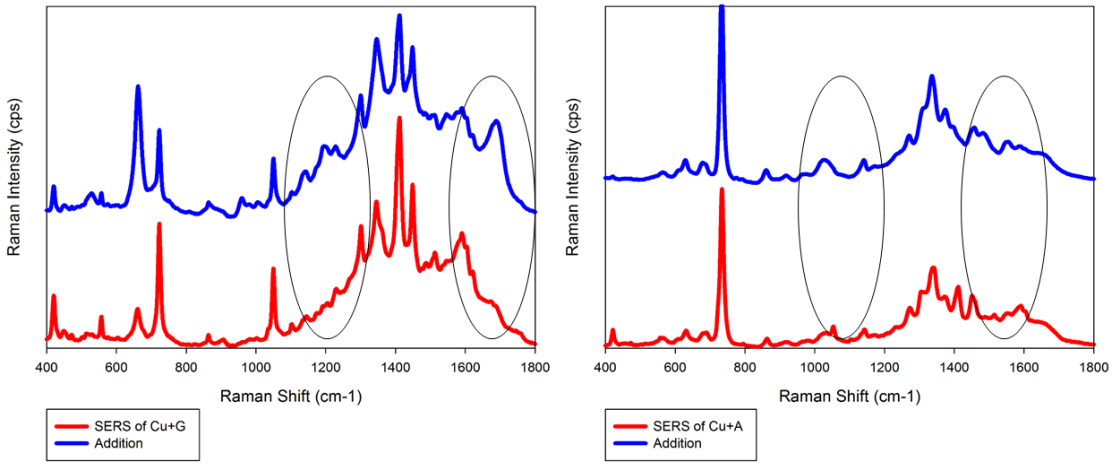


Figure 25. Surface-enhanced Raman spectra of $Cu(phen)_2CO_3(H_2O)_7$/ green (1) color with guanine (left) or adenine (right) by experimental addition (red) and adding two spectra (blue).

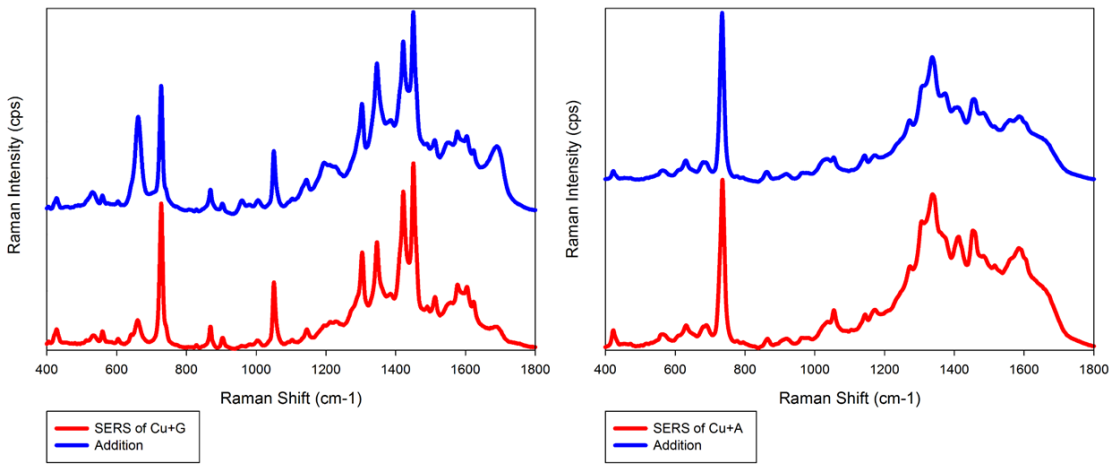


Figure 26. Surface-enhanced Raman spectra of $[Cu(phen)_2Cl]^+BF_4^-$/ green (2) color with guanine (left) or adenine (right) by experimental addition (red) and adding two spectra (blue).

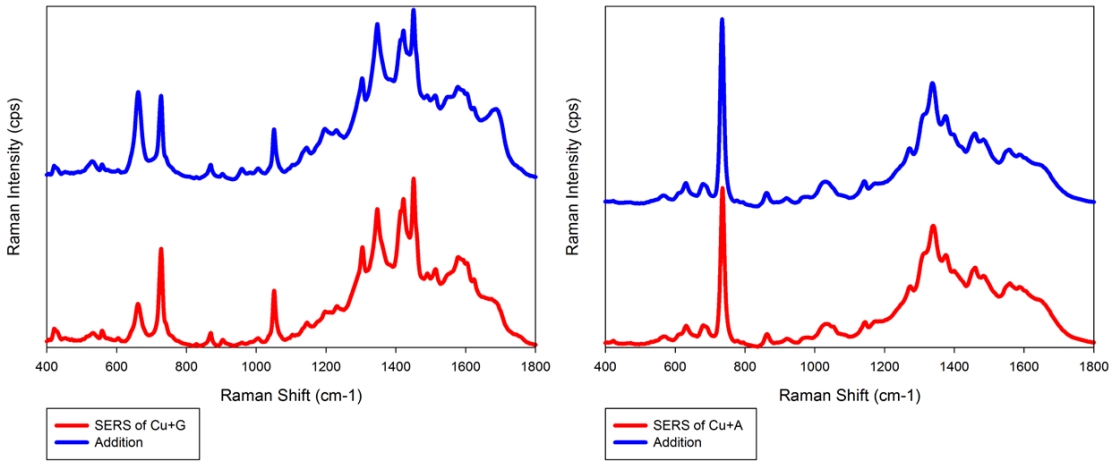


Figure 27. Surface-enhanced Raman spectra of $Cu(phen)_n$/ black color with guanine (left) or adenine (right) by experimental addition (red) and adding two spectra (blue).

As seen in Figures 24, 25, 26, and 27, the SERS spectra, by adding two spectra and experimental additions, shows the differences and similarities, particularly in the range 400 – 1800 $cm^{-1}$. In Figure 24 left, the SERS spectra of $[Cu_4(phen)_4(CH_3CN)_2(OH)_4]_4^+(BF_4^-)_4$/ blue color and guanine by adding two spectra and experimental addition show the difference in the regions of 1100 $cm^{-1}$ to 1300 $cm^{-1}$ and 1650 $cm^{-1}$ to 1750 $cm^{-1}$. Two humps appear at 1250 $cm^{-1}$ and 1700 $cm^{-1}$ in the physical addition spectrum, but they disappear in the experimental addition spectrum. In figure 24 right, the SERS spectra of $[Cu_4(phen)_4(CH_3CN)_2(OH)_4]_4^+(BF_4^-)_4$/ blue color and adenine, by adding two spectra and experimental addition, show the differences in the regions of 900 $cm^{-1}$ to 1200 $cm^{-1}$ and 1350 $cm^{-1}$ to 1700 $cm^{-1}$. In the experimental addition spectrum, the peak clusters are shown clearly, while in the physical addition spectrum, some peaks are shown. In Figure 25 left, the SERS spectra of $Cu(phen)_2CO_3(H_2O)_7$/ green (1) color and guanine, by adding two spectra and experimental addition, show the differences in the regions of 500 $cm^{-1}$ to 600 $cm^{-1}$, 900 $cm^{-1}$ to 1400 $cm^{-1}$, and 1500 $cm^{-1}$ to 1800 $cm^{-1}$. The resolved peaks at 1700 $cm^{-1}$, and peak clusters are not showing up in the experimental addition plotted spectra. In Figure 25 right, the SERS spectra of $Cu(phen)_2CO_3(H_2O)_7$/ green (1) color and adenine, by adding two spectra and experimental addition, show the differences in the regions of 900 $cm^{-1}$ to 1200 $cm^{-1}$ and 1400 $cm^{-1}$ to 1600 $cm^{-1}$. The resolved peaks are shown in the experimental addition plot. Among the graph of $[Cu(phen)_2Cl]^+BF_4^-$/ green (2) color or $Cu(phen)_n$/ black color and guanine or adenine in Figures 26 and 27, there are no noticeable differences between the experimental addition spectra and the physical addition spectra. The relative peak intensity differences might be seen. However, in the study of SERS, the positions of peaks give the meaning for vibrational spectra, while the intensity does not, since SERS intensity depends on the quality of absorbance and laser focusing.

When the comparison between adding two spectra and experimental additions are graphed and analyzed, only $[Cu_4(phen)_4(CH_3CN)_2(OH)_4]_4^+(BF_4^-)_4$/ blue color and $Cu(phen)_2CO_3(H_2O)_7$/ green (1) color are reported to suggest the differences. Further analysis needs to follow up to understand these spectral changes.

**THE EFFECTIVENESS OF AGGREGATION AGENT AND NANOPARTICLES**

The spectra were changed upon the addition of $[Cu_4(phen)_4(CH_3CN)_2(OH)_4]_4^+(BF_4^-)_4$/ blue color or $Cu(phen)_2CO_3(H_2O)_7$/ green (1) color to guanine or adenine. However, we could not conclude that the copper complexes had modified DNA bases. The spectral changes could come from many factors such as nanoparticles and aggregation agents. On the next stage of analysis, the effectiveness of nanoparticles and salt were considered. The study will eliminate the prospects that silver nanoparticles or $MgSO_4$ can react to copper complexes. The sample preparation for salt effect was the same as above, except 100 µL of salt was not added to the vials. The sample preparation for the nanoparticles effect was changing the amount of silver nanoparticles added. Copper complexes to nanoparticles were approximately 5:1, and viceversa.

- Copper complexes > Nanoparticles: 500 µL of copper complexes ($10^{-3}$ M) was combined with 100 µL of nanoparticles and 200 µL of $MgSO_4$.
- Copper complexes < Nanoparticles: 100 µL of copper complexes ($10^{-3}$ M) was combined with 500 µL of nanoparticles and 200 µL of $MgSO_4$.

The figures below demonstrate results on the effect of nanoparticles and salt. These works were conducted by SERS and UV-Vis techniques.

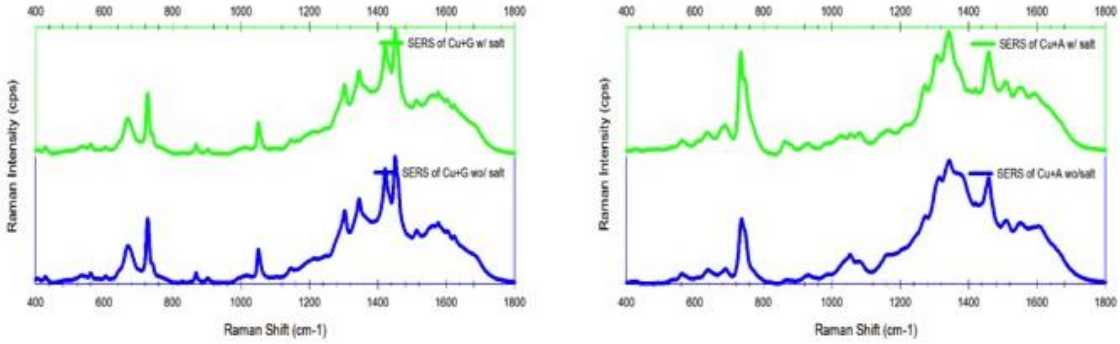


Figure 28. Surface-enhanced Raman spectra of $[Cu_4(phen)_4(CH_3CN)_2(OH)_4]_4^+(BF_4^-)_4$/ blue color interacted with guanine (left) or adenine (right) with the presence of $MgSO_4$ (green) or without the presence of $MgSO_4$ (blue); excitation laser, 780 nm; exposure time, 3 s; copper complexes concentration, $10^{-3}$ M.

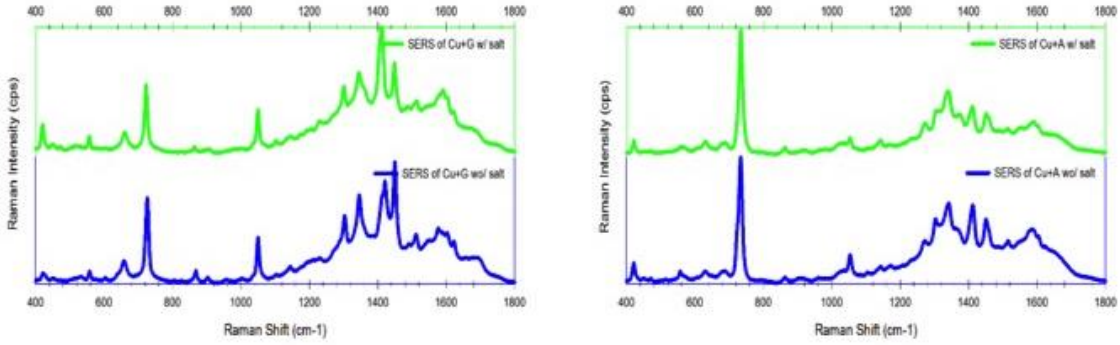


Figure 29. Surface-enhanced Raman spectra of $Cu(phen)_2CO_3(H_2O)_7$/ green (1) color interacted with guanine (left) or adenine (right) with the presence of $MgSO_4$ (green) or without the presence of $MgSO_4$ (blue); excitation laser, 780 nm; exposure time, 3 s; copper complexes concentration, $10^{-3}$ M.

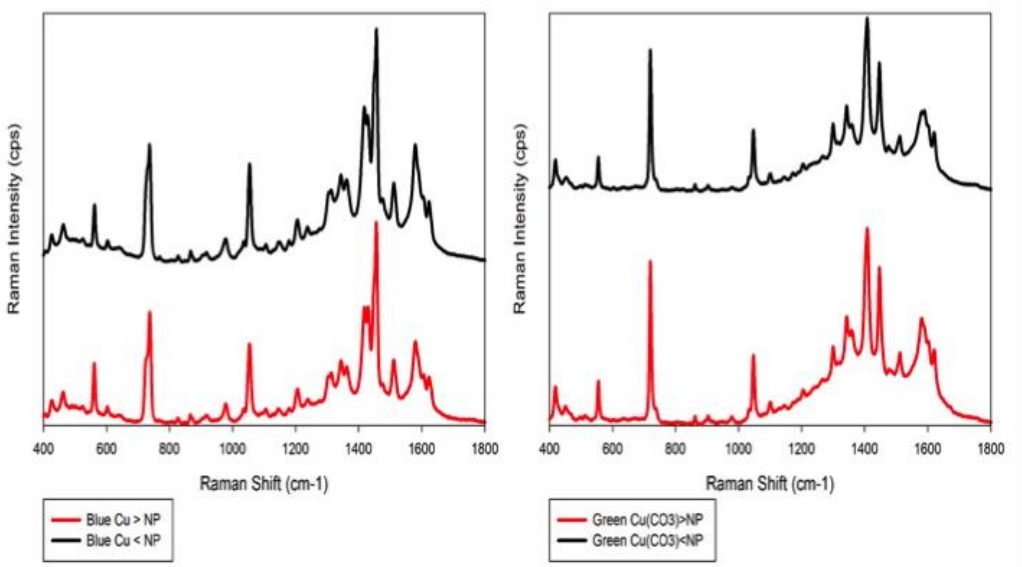


Figure 30. Surface-enhanced Raman spectra of $[Cu_4(phen)_4(CH_3CN)_2(OH)_4]_4^+(BF_4^-)_4$/ blue color (left) or $Cu(phen)_2CO_3(H_2O)_7$/ green (1) color adsorbed on silver surface, copper complexes to silver nanoparticles ratio 5:1 (red) and 1:5 (black); excitation laser, 780 nm; exposure time, 3 s; copper complexes concentration, $10^{-3}$ M.

Figures 28 and 29 above illustrate the results. Comparing two spectra with salt and without salt in $[Cu_4(phen)_4(CH_3CN)_2(OH)_4]_4^+(BF_4^-)_4$/ blue color, there are no differences among the spectra. There are also no differences in the spectra of $Cu(phen)_2CO_3(H_2O)_7$/ green (1) color. As observed, the vials, which had no salt, took longer to aggregate and seemed to have less amount of aggregation. In the study of the nanoparticles effect, the ratio of copper complexes to silver nanoparticles was taken into account in order to identify if silver nanoparticles can react to copper complexes. As seen in Figure 30, the nature of the adsorption of copper complexes on the silver surface was displayed. There are absolutely no differences between the two spectra; even the silver nanoparticles were adding more or less than copper complexes. In general, no effectiveness was found in the presence of silver nanoparticles or salt $MgSO_4$.

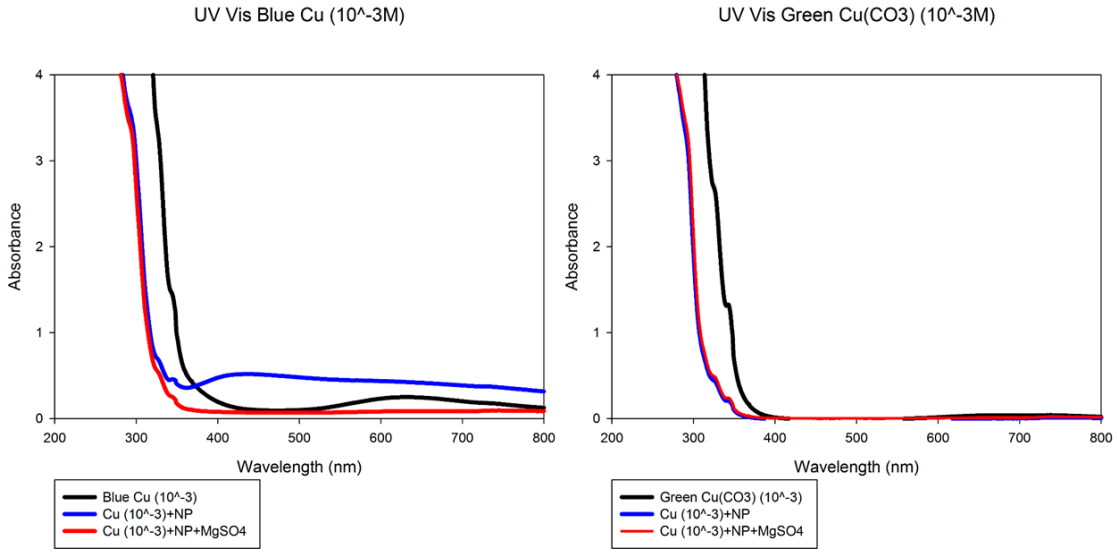


Figure 31. UV-Vis spectra of $[Cu_4(phen)_4(CH_3CN)_2(OH)_4]_4^+(BF_4^-)_4$/ blue color (left) or $Cu(phen)_2CO_3(H_2O)_7$/ green (1) color (right), before the addition of silver nanoparticles (black), after the addition of silver nanoparticles (blue), and then $MgSO_4$ (red).

Figure 31 shows the absorbance of copper complexes and nanoparticles. As seen, both copper complexes have the maximum absorbance near 300 nm. The silver nanoparticles, which were made basing on Lee and Meisel protocol, have the absorbance near 400 – 500 nm[33].

**THE ANALYSIS OF SPECTRAL CHANGES**

Since four newly synthesized copper complexes were investigated on guanine or adenine, the analysis was put through to conceivably compare the differences when adding two spectra and experimental additions. The $[Cu_4(phen)_4(CH_3CN)_2(OH)_4]_4^+(BF_4^-)_4$/ blue color and $Cu(phen)_2CO_3(H_2O)_7$/ green (1) color showed the spectral changes, while the $[Cu(phen)_2Cl]^+BF_4^-$/ green (2) color and $Cu(phen)_n$/ black color did not. The effectiveness of nanoparticles and salts were taken into account to recognize these changes. However, no differences were found when the reactions were changing in conditions. This suggests that $[Cu_4(phen)_4(CH_3CN)_2(OH)_4]_4^+(BF_4^-)_4$/ blue color or $Cu(phen)_2CO_3(H_2O)_7$/ green (1) color could modify DNA bases. The next part of the project was to explore the spectral features of guanine or adenine before and after adding the copper complexes.

The SERS spectra of the reaction of copper complexes and DNA bases are graphed and illustrated in Figures 32 and 33 together with the SERS spectra DNA bases.

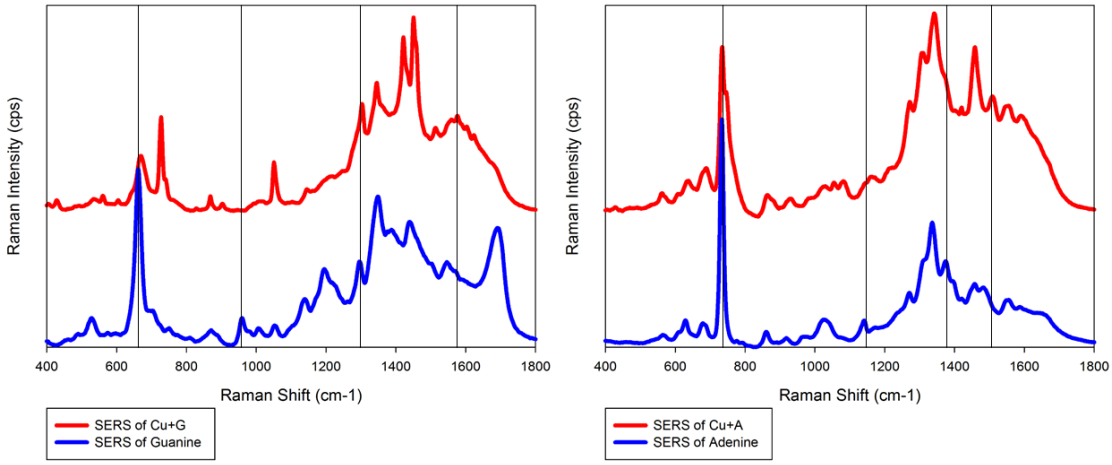


Figure 32. Surface-enhanced Raman spectra of $[Cu_4(phen)_4(CH_3CN)_2(OH)_4]_4^+(BF_4^-)_4$/ blue color interacted with guanine (left, red) vs. guanine (left, blue) and $[Cu_4(phen)_4(CH_3CN)_2(OH)_4]_4^+(BF_4^-)_4$/ blue color interacted with adenine (right, red) vs. adenine (right, blue); excitation laser, 780 nm; exposure time, 3 s; guanine concentration, $10^{-3}$ M; copper complexes concentration $10^{-3}$ M.

From Figure 32 left, there are many spectral changes before and after adding $[Cu_4(phen)_4(CH_3CN)_2(OH)_4]_4^+(BF_4^-)_4$/ blue color to guanine. The peak at 730 $cm^{-1}$ does not develop on guanine spectra, but it is seen on the spectra of modified guanine. The peak observed at 528 $cm^{-1}$, 1140 $cm^{-1}$, 1200 $cm^{-1}$ and 1690 $cm^{-1}$ on the SERS spectrum of guanine disappeared on the SERS spectrum of the complex interacted with guanine. The peaks at 662 $cm^{-1}$, 1296 $cm^{-1}$, 1349 $cm^{-1}$, 1388 $cm^{-1}$, and 1439 $cm^{-1}$ shifted to 669 $cm^{-1}$, 1303 $cm^{-1}$, 1345 $cm^{-1}$, 1422 $cm^{-1}$, and 1451 $cm^{-1}$ upon the presence of the complexes. Also, the relative peaks from 1300 $cm^{-1}$ to 1500 $cm^{-1}$ are different between two spectra. The cluster of peaks in the range of 1500 $cm^{-1}$ to 1700 $cm^{-1}$ is not resolved in the SERS spectrum of $[Cu_4(phen)_4(CH_3CN)_2(OH)_4]_4^+(BF_4^-)_4$/ blue color interacted with guanine. The peak at 1195 $cm^{-1}$ and 1053 $cm^{-1}$ in guanine indicate the stretching at position N3 and N7, respectively. These peaks disappeared when the complex was added to guanine. The binding of copper and nitrogen could occur at these positions. From Figure 32 right,

the SERS spectrum between adenine and $[Cu_4(phen)_4(CH_3CN)_2(OH)_4]_4^+(BF_4^-)_4$/ blue color interacted with adenine show some similarities. Two scans from 400 $cm^{-1}$ to 750 $cm^{-1}$ show no new peaks or any shifts. The cluster of peaks in both spectra from 850 $cm^{-1}$ to 1250 $cm^{-1}$ and 1500 $cm^{-1}$ to 1700 $cm^{-1}$ are not resolving. The peak at 1375 $cm^{-1}$ is the bending and stretching mode at position N9. It disappears in the presence of the complex. The peaks at 1270 $cm^{-1}$ and 1340 $cm^{-1}$ have no shift in both spectra. However, the appearance of the peak at 1460 $cm^{-1}$ is found when $[Cu_4(phen)_4(CH_3CN)_2(OH)_4]_4^+(BF_4^-)_4$/ blue color were added to adenine. This peak associates with stretching C2-N3 and N1-C6, bending C2-H, and scissoring $NH_2$.

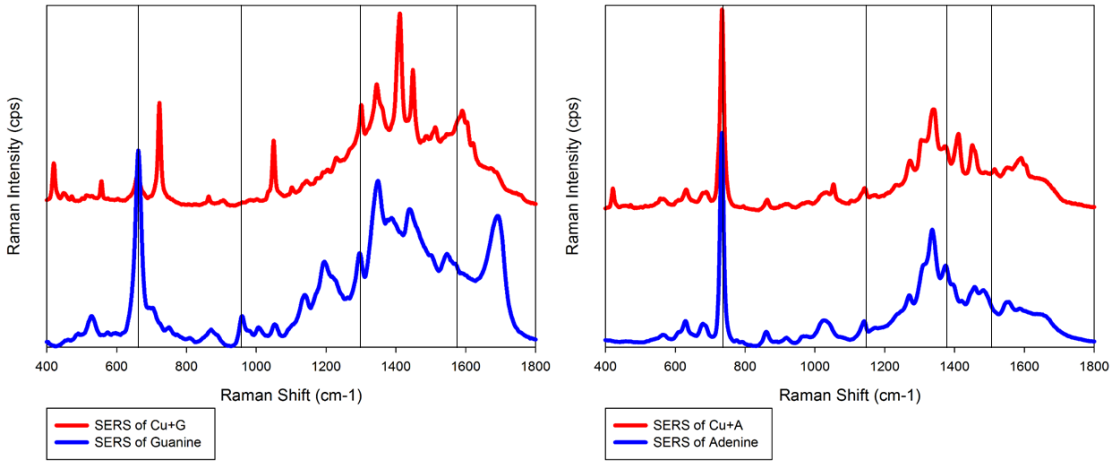


Figure 33. Surface-enhanced Raman spectra of $Cu(phen)_2CO_3(H_2O)_7$/ green (1) color interacted with guanine (left, red) vs. guanine (left, blue) and $Cu(phen)_2CO_3(H_2O)_7$/ green (1) color interacted with adenine (right, red) vs. adenine (right, blue); excitation laser, 780 nm; exposure time, 3 s; guanine concentration, $10^{-3}$ M; copper complexes concentration $10^{-3}$ M.

In Figure 33 left, the spectra between guanine and $Cu(phen)_2CO_3(H_2O)_7$/ green (1) color interacted with guanine shows some differences. The peaks at 420 $cm^{-1}$ and 720 $cm^{-1}$ exist in the SERS spectrum of $Cu(phen)_2CO_3(H_2O)_7$/ green (1) color interacted with guanine, but they are not seen in the SERS spectrum of guanine. The relative peaks at 662 $cm^{-1}$ pronounced the signal of 6-ring breathing; 5-ring deforming and wagging $NH_2$ are different between two spectra. Alternatively, the cluster of peaks such as 800 $cm^{-1}$ to 1300 $cm^{-1}$ is not dominant in the SERS

spectrum of $Cu(phen)_2CO_3(H_2O)_7$/ green (1) color interacted with guanine. The peak at 1195 $cm^{-1}$ associates with stretching at position N7. The region from 1300 $cm^{-1}$ to 1500 $cm^{-1}$ shows shifts. This region indicates the bending at N1-H, N10-H, C8-H and stretching at C2-N10, C-N ring stretching. Also, the cluster of peaks from 1500 $cm^{-1}$ to 1700 $cm^{-1}$ in the spectrum of DNA bases-complexes is not determined. The peak observed at 1690 $cm^{-1}$, which is assigned to carbonyl stretching absorption, is not recognized in the modified guanine spectrum. Looking at Figure 33 right, there are similarities near the region of 400 $cm^{-1}$ to 800 $cm^{-1}$, except the peak at 420 $cm^{-1}$ is arisen in the SERS spectrum of $Cu(phen)_2CO_3(H_2O)_7$/ green (1) color interacted with adenine. The cluster of peaks from 800 $cm^{-1}$ to 1200 $cm^{-1}$ and 1500 $cm^{-1}$ to 1700 $cm^{-1}$ are not resolute in both spectra. The peaks at 1270 $cm^{-1}$ and 1340 $cm^{-1}$ also do not contribute to any changes. However, two new peaks are seen at 1410 $cm^{-1}$ and 1450 $cm^{-1}$ in the SERS spectrum of $Cu(phen)_2CO_3(H_2O)_7$/ green (1) color interacted with adenine. The signal of scissoring $NH_2$, bending C2-H, and stretching C2-N3, N1-C6 are found in the region 1400 $cm^{-1}$ – 1800 $cm^{-1}$.

**CONCLUSION**

The binding activities to purine bases of a series of new copper complexes containing 1,10-phenanthroline have been investigated using the SERS technique. The confirmational changes of SERS experimentation took place when the condition was at 1:1 ratio of copper complexes to DNA bases, $10^{-3}$ M concentration of copper complexes and DNA bases, and incubation time of 24 hours. Among four new copper complexes, $[Cu_4(phen)_4(CH_3CN)_2(OH)_4]_4^+(BF_4^-)_4$/ blue color and $Cu(phen)_2CO_3(H_2O)_7$/ green (1) color are known to possibly modify DNA bases through spectral analysis. The other copper complexes such as $[Cu(phen)_2Cl]^+BF_4^-$/ green (2) color and $Cu(phen)_n$/ black color did not react to either guanine or adenine. The SERS experiments required the use of $MgSO_4$ and silver nanoparticles; however, these agents did not affect to the binding of copper complexes to the bases.

The SERS study of the DNA-copper complex interactions is onerous work, because a lot of experiments and analysis have to be attained to find out the effectiveness factors such as metal adsorption surface and aggregation agent. The binding actions of $[Cu_4(phen)_4(CH_3CN)_2(OH)_4]_4^+(BF_4^-)_4$/ blue color and $Cu(phen)_2CO_3(H_2O)_7$/ green (1) color to guanine or adenine can be compared in future inquiries. Through a comprehensive analysis, the complexes of $[Cu_4(phen)_4(CH_3CN)_2(OH)_4]_4^+(BF_4^-)_4$/ blue color and $Cu(phen)_2CO_3(H_2O)_7$/ green (1) color show more observable spectral changes than cisplatin or carboplatin. Theoretical calculations should be performed to understand the binding mode of the copper complexes to DNA.

# CHAPTER VIII

## CLOSING REMARKS AND FUTURE WORKS

As a whole, this thesis has mainly focused on the mechanism of anticancer activity of platinum-based drugs and newly synthesized copper complexes. Such conditions such as ratio, concentration, and incubation time were attempted. SERS is a powerful technique that was employed to study the interaction of metal-based complexes with DNA bases. Likewise, other spectroscopic techniques in particular normal Raman and IR spectroscopy were used to determine the molecular vibrations of new copper complexes.

This research provided the significance of future research. Since the clinical success of cisplatin and carboplatin has placed metal-based drugs as potential anticancer agents. The new drugs design has been under investigation to overcome the shortcomings of cisplatin such as toxicity and drug resistance. The development will continue to be a main subject in the inorganic as well as physical chemistry.

REFERENCES


(1) Patil, Y. P.; Pawar, S. H.; Jadhav, S.; Kadu, J. S. Biochemistry of Metal Absorption in Human Body: Reference to Check Impact of Nano Particles on Human Being." *International Journal of Scientific and Research Publications* **2013**, *3*, 1-5.

(2) Miessler, G. L.; Tarr, D. A. *Inorganic Chemistry*; 3rd ed.; Pearson: London, UK, 2004.

(3) Frezza, M.; Hindo, S.; Chen, D.; Davenport, A.; Schmitt, S.; Tomco, D., Dou, Q. P. Novel Metals and Metal Complexes as Platforms for Cancer Therapy. *Curr. Pharm. Des*. **2010**, *16*, 1813-1825.

(4) Kauffman, G. B. Michele Peyrone (1813-1883), Discoverer of Cisplatin. *Platinum Metals Rev.* **2010**, *54*, 250-256.

(5) Kauffman, G. B. Alfred Werner's Research on The Platinum Metals. *Platinum Metals Rev.* **1997**, *41*, 34-40.

(6) Kelland, L. The Resurgence of Platinum-Based Cancer Chemotherapy. *Nat Rev Cancer.* **2007**, *7*, 573-84.

(7) Dilruba, S.; Kalayda, G. V. Platinum-Based Drugs: Past, Present and Future. *Cancer chemotherapy and pharmacology* **2016**, *77*, 1103-1124.

(8) Fonseca de Souca, G.; Wlodarczyk, S. R.; Monteiro, G. Carboplatin: Molecular Mechanisms of Action Associated with Chemoresistance. *Brazilian Journal of Pharmaceutical Sciences* **2014**, *50*, 693-701

(9) Lokich, J. What is The "Best" Platinum: Cisplatin, Carboplatin, or Oxaliplatin? *Cancer investigation* **2001**, *19*, 756-760.

(10) Johnstone, T. C.; Suntharalingam, K.; Lippard, S. J. Third Row Transition Metals for the Treatment of Cancer. *Phil. Trans. R. Soc. A.* **2015**, *373*, 1-12.

(11) Kelland, L. R.; Farrell, N. *Platinum-Based Drugs in Cancer Therapy*; 1st[t] ed.; Human Press: Totowa, NJ, USA, 2000.

(12) Di Pasqua, A. J.; Goodisman, J.; Dabrowiak, J. C. Understanding How the Platinum Anticancer Drug Carboplatin Works: From the Bottle to The Cell. *Inorganica Chimica Acta* **2012**, *389*, 29-35.

(13) Ochiai, E. *Bioinorganic chemistry: an introduction*; 1st ed.; Allyn & Bacon: Boston, MA, USA, 1977.

(14) Marzano, C.; Pellei, M.; Tisato, F.; Santini, C. Copper Complexes as Anticancer Agents. *Anti-Cancer Agents in Medicinal Chemistry* **2009**, *9*, 185-211.

(15) Osredkar, J.; Sustar, N. Copper and Zinc, Biological Role and Significance of Copper/Zinc Imbalance. *Journal of Clinical Toxicology* **2011**, *S:3*, 1-18.

(16) Brown D. H.; Smith W. E.; Teape J. W.; Lewis A. J. Antiinflammatory Effects of Some Copper Complexes. *J. Med. Chem*. **1980**, *23*, 729-734.

(17) Jackson, G. E.; Mkhonta-Gama, L.; Voyé, A.; Kelly, M. Design of Copper-Based Anti-Inflammatory Drugs. *Journal of Inorganic Biochemistry* **2000**, *79*, 147-152.

(18) Iakovidis, I.; Delimaris, I.; Piperakis, S. M. Copper and Its Complexes in Medicine: A biochemical Approach. *Molecular Biology International* **2011**, *2011*, 1-13.

(19) Greenaway, F. T.; Hahn, J. J.; Xi, N.; Sorenson, J. R. Interaction of Cu(II) 3,5-Diisopropylsalicylate with Human Serum Albumin - An Evaluation of Spectroscopic Data. *Biometals* **1998**, *11*, 21-26.

(20) Wu, J.; Chen, W.; Yin, Y.; Zheng, Z.; Zou, G. Probing the Cell Death Signaling Pathway of HepG2 Cell Line Induced by Copper-1,10-Phenanthroline Complex. *Biometals* **2014**, *27*, 445-458.

(21) Sigman, D. S.; Graham, D. R.; D'Aurora, V.; Stern, A. M. Oxygen-Dependent Cleavage

of DNA by the 1,10-Phenanthroline.Cuprous Complex. Inhibition of *Escherichia coli* DNA Polymerase I. *J. Biol. Chem.* **1979**, *254*, 2269-2272.

(22) Nakamoto, K.; Tsuboi, M.; Strahan, G. D. *Drug-DNA Interactions Structures and Spectra*; 1st ed.; John Wiley & Son, Inc: Hoboken, NJ, USA, 2008.

(23) García-Ramos, J. C.; Galindo-Murillo, R.; Cortés-Guzmán, F.; Ruiz-Azuara, L. Metal-Based Drug-DNA Interactions. *J. Mex. Chem. Soc.* **2013**, *57*, 245-259.

(24) Baraldi, P. G.; Bovero, A.; Fruttarolo, F.; Preti, D.; Tabrizi, M. A.; Pavani, M. G.; Romagnoli, R. DNA Minor Groove Binders as Potential Antitumor and Antimicrobial Agents. *Med. Res. Rev*. **2004**, *24*, 475–528.

(25) Mu-Hyun, B.; Friesner, R. A.; Lippard, S. J. Theoretical Study of Cisplatin Binding to Purine Bases: Why Does Cisplatin Prefer Guanine over Adenine? *J. Am. Chem. Soc.* **2003**, *125*, 14082-14092.

(26) Chakravarty, A. R. Photocleavage of DNA by Copper(II) Complexes. *J. Chem. Sci*. **2006**, *118*, 443-453.

(27) Sigman, D. S. Chemical Nucleases. *Biochemistry* **1990**, *29*, 9097-9105.

(28) Sigman, S. D.; Mazumder, A.; Perrin, D. M. Chemical nucleases. *Chem. Rev*. **1993**, *93*, 2295-2316.

(29) Skoog, D. A.; Holler, F. J.; Nieman, T. A. *Principles of Instrumental Analysis*; 5th ed.; Wadsworth Publishing Co Ins: Belmont, CA, USA, 1997.

(30) Ru, E. L.; Etchegoin, P. *Principles of Surface Enhanced Raman Spectroscopy and related plasmonic effects*; 1st ed.; Elsevier: Oxford, UK, 2009.

(31) Sharma, B.; Frontiera, R. R.; Henry, A. I.; Ringe, E.; Van Duyne, R. P. SERS: Materials, Applications, and The Future. *materialstoday* **2012**, *15*, 16-25.

(32) Sirajuddin, M.; Ali, S.; Badshah, A. Drug-DNA Interactions and Their Study by UV-

Visible, Fluorescence Spectroscopies and Cyclic Voltammetry. *Journal of Photochemistry and Photobiology B: Biology* **2013**, *124*, 1-19.

(33) Lee, P. C.; Meisel, D. Adsorption and Surface-Enhanced Raman of Dyes on Silver and Gold Sols. *Journal of Physics and Chemistry* **1982**, *86*, 3391-3385.

(34) Oh, W. S.; Kim, M. S.; Suh, S. W. Surface-Enhanced Raman Scattering (SERS) of Nucleic Acid Components in Silver Sol: Guanine Series. *J. Raman Spectrosc*. **1987**, *18*, 253.

(35) Giese, B.; McNaughton, D. Density Functional Theoretical (DFT) and Surface-Enhanced Raman Spectroscopic Study of Guanine and Its Alkylated Derivatives. *Phys. Chem. Chem. Phys*. **2002**, *4*, 5171-5182.

(36) Jang, Y. H.; Goddard III, W. A.; Noyes, K. T.; Sowers, L. C.; Hwang, S.; Chung, D. S. p$K_a$ Values of Guanine in Water: Density Functional Theory Calculations Combined with Poisson-Boltzmann Continuum-Solvation Model. *J. Phys. Chem. B.* **2003**, *107*, 344-357.

(37) Petrović, M.; Todorović, D. Biochemical and Molecular Mechanisms of Action of Cisplatin in Cancer Cells. *Facta Universitatis, Series: Medicine & Biology* **2016**, *18*, 12-18.

(38) Jangir, D. K.; Mehrotra, R. Raman Spectroscopic Evaluation of DNA Adducts of a Platinum Containing Anticancer Drugs. *Spectrochimica Acta Part A: Molecular and Biomolecular Spectroscopy* **2014**, *130*, 386-389.

(39) Giese, B.; McNaughton, D. Interaction of Anticancer Drug Cisplatin with Guanine: Density Functional Theory and Surface-Enhanced Raman Spectroscopy Study. *Biopolymers* **2003**, *72*, 472-489.

(40) Ndagi, U.; Mhlongo, N.; Soliman, M. E. Metal Complexes in Cancer Therapy – An Update from Drug Design Perspective. *Drug Design, Development and Therapy* **2017**,

*11*, 599-616.

(41) Hu, J.; Liao, C.; Mao, R.; Zhang, J.; Zhao, J.; Gu, Z. DNA Interactions and *In Vitro* Anticancer Evaluations of Pyridine-Benzimidazole-Based Cu Complexes. *MedChemComm*. **2018**, *9*, 337-343.

(42) Adsule, S.; Barve, V.; Chen, D.; Fakhara, A.; Dou, Q. P.; Padhye, S.; Sarkar, F. H. Novel Schiff Base Copper Complexes of Quinoline-2 Carboxaldehyde as Proteasome Inhibitors in Human Prostate Cancer Cells. *J. Med. Chem.* **2006**, *49*, 7242-7246.

(43) Ma, Z. Y.; Shao, J.; Bao, W. G.; Qiang, Z. Y; Xu, J. Y. A Thiosemicarbazone Copper(II) Complex as A Potential Anticancer Agent. *Journal of Coordination Chemistry* **2015**, *68*, 277-294.

(44) Accorsi, G.; Listorti, A.; Yoosaf, K.; Armaroli, N. 1,10-Phenanthrolines:Versatile Building Blocks for Luminescent Molecules, Materials and Metal Complexes. *Chemical Society Reviews* **2009**, *38*, 1690-1700.

(45) Chen, C. H. B.; Mazumder, A.; Constant, J. F.; Sigman, D. S. Nuclease Activity of 1,10-Phenanthroline-Copper. New Conjugates with Low Molecular Weight Targeting Ligands. *Bioconjugate Chem*. **1993**, *4*, 69-77.

(46) Madzharova, F.; Heiner, Z.; Guhlke, M.; Kneipp, J. Surface-Enhanced Hyper-Raman Spectra of Adenine, Guanine, Cytosine, Thymine, and Uracil. *J. Phys. Chem. C.* **2016**, *120*, 15415-15423.

(47) Kagawa, T. F.; Geierstanger, B. H.; Wang, A. H. J.; Ho, P. S. Covalent Modification of Guanine Bases in Double-strand DNA The 1.2-A Z-DNA Structure of d(CGCGCG) In The Presence of $CuCl_2$. *The Journal of Biological Chemistry* **1991**, 266, 20175-20184.

(48) Choquesillo-Lazarte, D.; Brandi-Blanco, M.; García-Santos, I.; González-Pérez, J. M.; Castiñeras, A.; Niclós-Gutiérrez, J. Interligand Interactions Involved in The Molecular

Recognition Between Copper(II) Complexes and Adenine or Related Purines. *Coordination Chemistry Reviews* **2008**, *252*, 1241-1256.